PART IV

INERTIAL MEASUREMENT UNITS AND PULSE TORQUING

by

John E. Miller

JOHN E. MILLER

Deputy Associate Director, Instrumentation Laboratory
Massachusetts Institute of Technology

John E. Miller, Deputy Associate Director of Instrumentation Laboratory, Massachusetts Institute of Technology, heads the Laboratory group that is developing the inertial measurement unit for the Project Apollo spacecraft guidance system.

Mr. Miller was born April 30, 1925, at Aberdeen, S. D., and was graduated from high school there in 1943. He served in the U. S. Army from 1943 to 1945 prior to appointment to the United States Military Academy, West Point, N. Y., where he was graduated in 1949.

Mr. Miller served in the U. S. Air Force from 1949 to 1958 and during this period was sent to M. I. T. for graduate study. He was awarded the M. S. degree in instrumentation in 1953. Also while serving as an Air Force officer, Mr. Miller taught inertial navigation and automatic control at the Air Force Institute of Technology, Dayton, O.

He joined the Instrumentation Laboratory in 1959 and initially worked on the development of accelerometers used in the Mark II guidance system the Laboratory designed for the Navy's Polaris missile.

Part IV

INERTIAL MEASUREMENT UNITS AND PULSE TORQUING

CHAPTER IV-1

THE APOLLO INERTIAL MEASUREMENT UNIT

INTRODUCTION

The Inertial Measurement Unit, IMU, provides three fundamental functions in a space guidance system. It established a non-rotating computing coordinate frame oriented to a desired inertial reference such that acceleration is measured in that frame. It provides information to a guidance computer of the orientation of that coordinate frame with respect to the control member, the spacecraft. It provides a measure of the specific force of the spacecraft (usually the integral of the specific force) in suitable form to the guidance computer.

The Apollo IMU is a three degree of freedom gimbal system utilizing integrating gyroscopes to detect angular deviations of the stable member with respect to inertial space, and to provide along with their servo electronics the establishment of a non-rotating member. On this stable member are three accelerometers in an orthogonal triad. The accelerometers are single degree of freedom pendulums with a digital pulse restraining system. Angle information as to the orientation of the computing coordinate frame, stable member, with respect to the navigation base is derived from a two speed resolver system mounted on each axis of the IMU. This resolver system provides knowledge of the stable member to both the astronaut and to the computer: to the astronaut by the means of a ball indicating system with resolvers servo controlled to follow the resolvers on the IMU. The ball has the same gimbal order as the IMU. The same resolver system by means of a Coupling Data Unit, CDU, provides to the computer quantized angle increments for changes in gimbal angles. The CDU couples angle information to and from the guidance computer, performing both analog to digital and digital to analog conversion.

Thermal and Mechanical - The Apollo Inertial Measurement Unit (IMU) is a three degree of freedom gimbaled system. The reasons for using this inertial measurement configuration have been previously stated. The IMU is described from the stable member to the case using Figure IV-1. The inertial components are (3) three single-degree-of-freedom Inertial Reference Integrating Gyroscopes

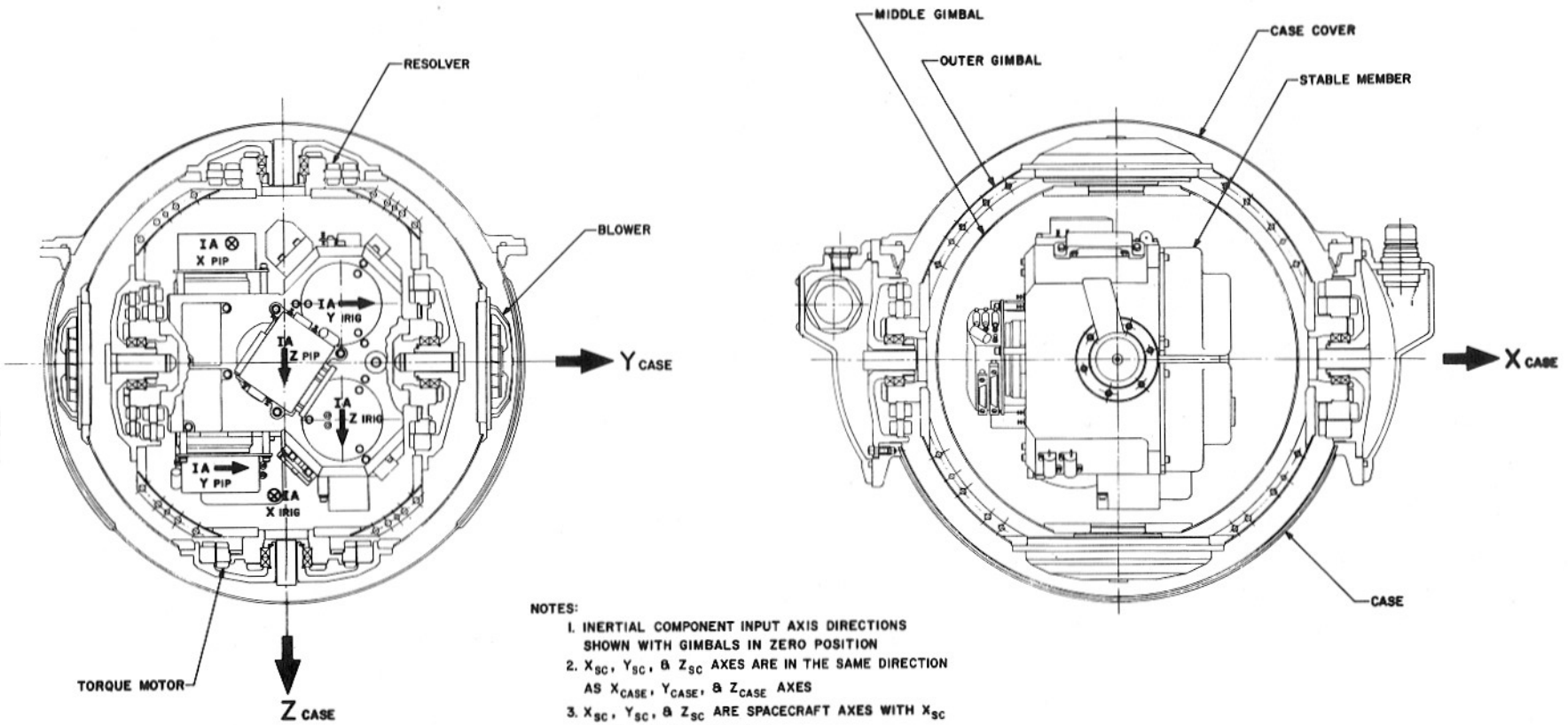

NOTES:

1. INERTIAL COMPONENT INPUT AXIS DIRECTIONS SHOWN WITH GIMBALS IN ZERO POSITION
2. X_{SC}, Y_{SC}, & Z_{SC} AXES ARE IN THE SAME DIRECTION AS X_{CASE}, Y_{CASE}, & Z_{CASE} AXES
3. X_{SC}, Y_{SC}, & Z_{SC} ARE SPACECRAFT AXES WITH X_{SC} ALONG THRUST DIRECTION

Fig. IV-1 12.5 IMU

(IRIG) and (3) three single-degree-of-freedom Pulsed Integrating Pendulums (PIP). These components are mounted on the inner member which is referred to as the stable member. It is the member which will be non-rotating with respect to the fixed stars except by the drift of the gyroscopes. The stable member also contains necessary electronics. Three degrees of freedom are obtained by coupling the stable member to a middle gimbal by means of an intergimbal assembly to provide one axis of rotation. Likewise a degree of freedom is provided between the middle and the outer gimbal and the outer gimbal and the case. Mounting pads are used as a means of precision alignment of the case onto the navigation base.

The gyroscopes and accelerometers are temperature controlled. The case of the IMU provides a hermetically sealed environment containing air at atmospheric pressure with leak rates less than 10^{-5} CC of He/sec equivalent. There is in the case an integral coolant passage for a heat sink. This integral coolant passage is formed by placing a pattern on a sheet of aluminum. This sheet of aluminum is roll bonded to another sheet except in the area of the pattern where no bonding takes place. The piece or case is formed and machined to the proper dimensions. The coolant passage is then inflated using air to form a coolant passage where the pattern has been placed. This provides a means of making a leak free integral coolant passage over a spherical surface. Water and glycol at 7^{o}C from the spacecraft coolant system is circulated at a rate of 15 Kg/hour and the pressure drop in the IMU is less than 703 Kg/M^2. The required operation of the IMU is for ambient pressure of zero for 14 days and environmental extremes from -18^{o}C to $+65^{o}$C. It may see these ambient structure temperatures depending upon orientation of the spacecraft with respect to the sun. The temperature of the gyroscopes and accelerometers is controlled by means of a thermostatic control system. Heat flow is from the stable member to the case and coolant. Around the stable member is a dead air space. The gyroscopes are controlled to 57^{o}C and the accelerometers to 54^{o}C. The major source of power is in the gyroscope wheels with smaller amounts in electromagnetic components such as torquers. A pair of blowers on the outer gimbal provide heat transfer by moving air over the middle gimbal and the case. There is insulation over the case that is shown in Figure IV-2 primarily because the case will be below the dew point. This is particularly true at the launch at Cape Kennedy. A mercury thermostat senses the stable member temperature by being mounted on the appropriate position of the stable member. A single thermostat is used to control the temperature of six inertial components. The thermostat energizes an end-mount heater on the pendulum, and end-mount heaters on each end of each gyro, and two stable member heaters. The inertial components have a vacuum shroud around the cylindrical wall to prevent circumferential gradients. All heat flow is thus axial which is

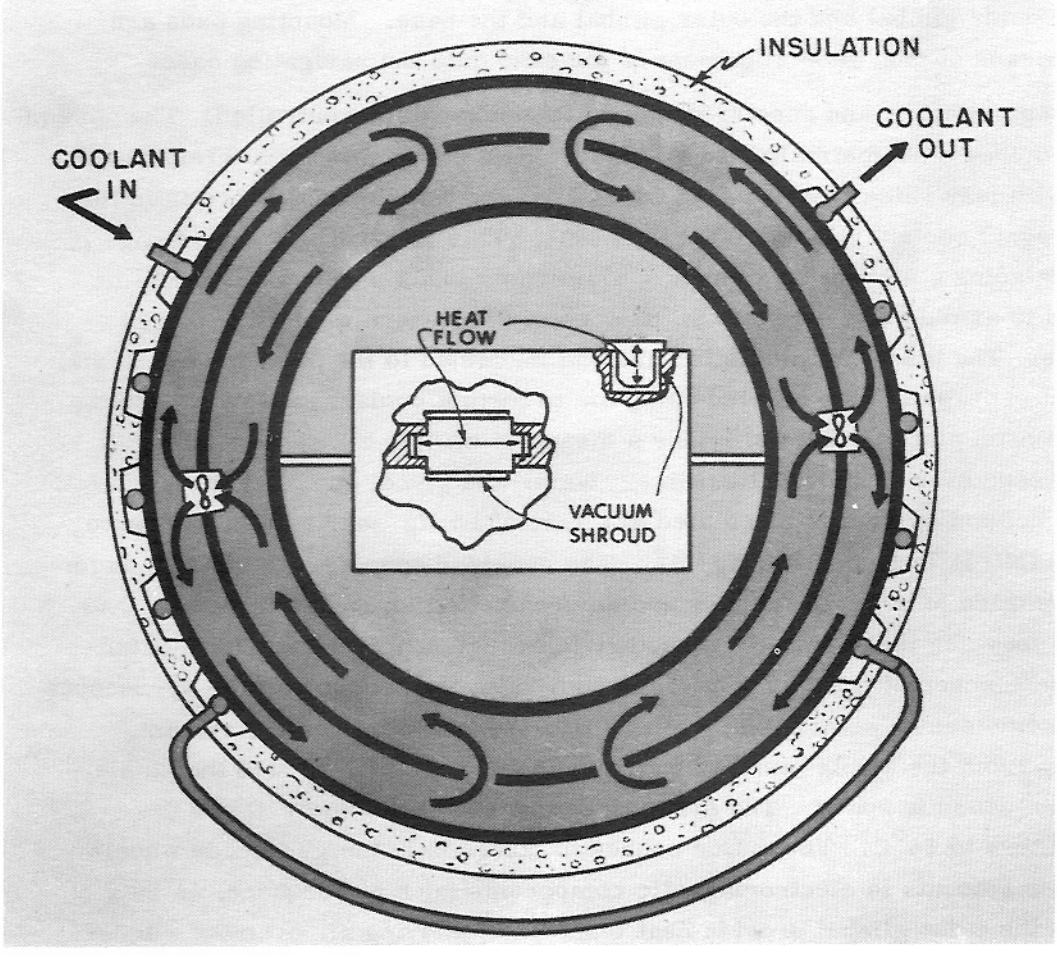

Fig. IV-2 IMU Heat Transfer Diagram

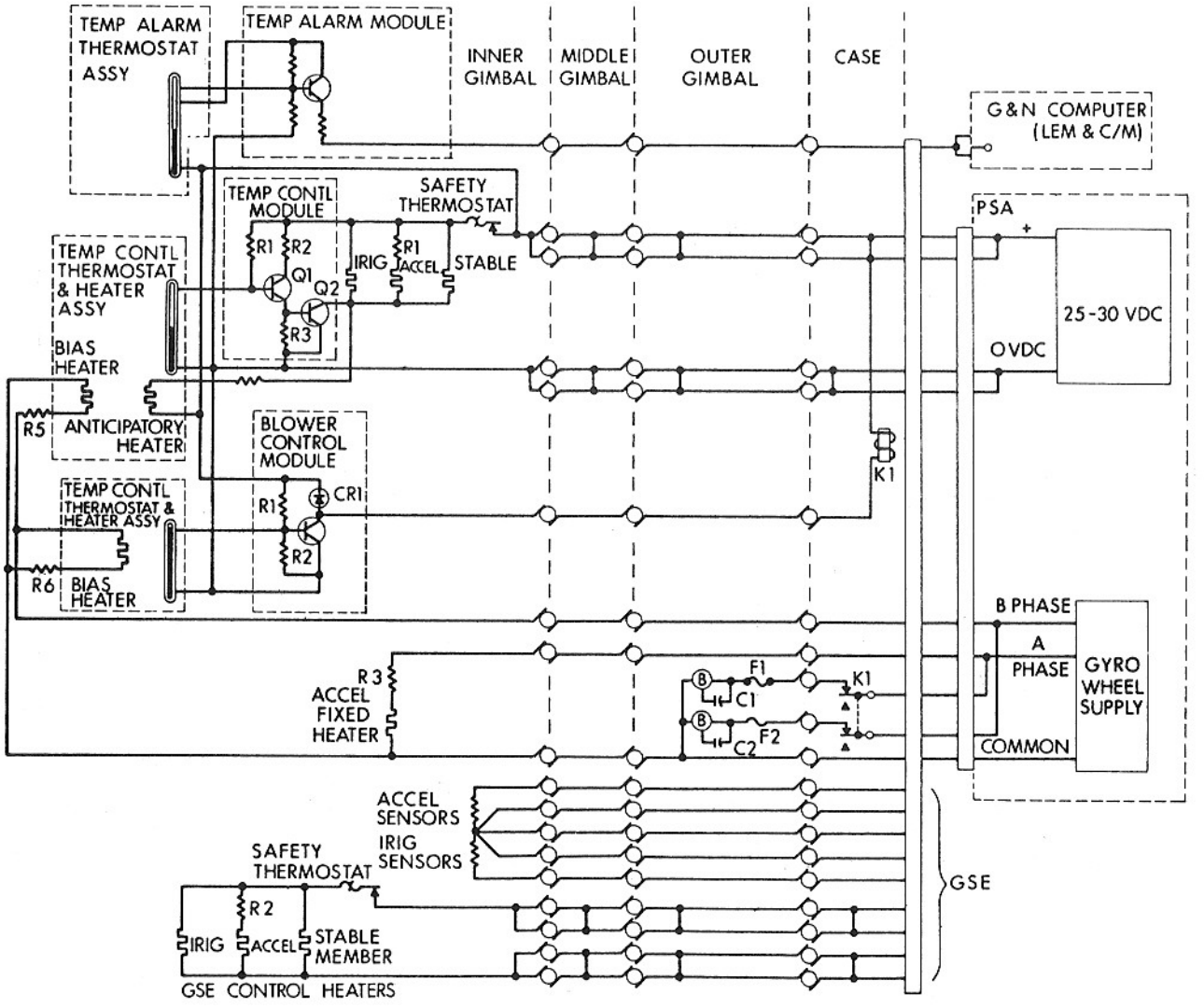

Fig. IV-3 Block II IMU Temperature Control System Schematic Diagram

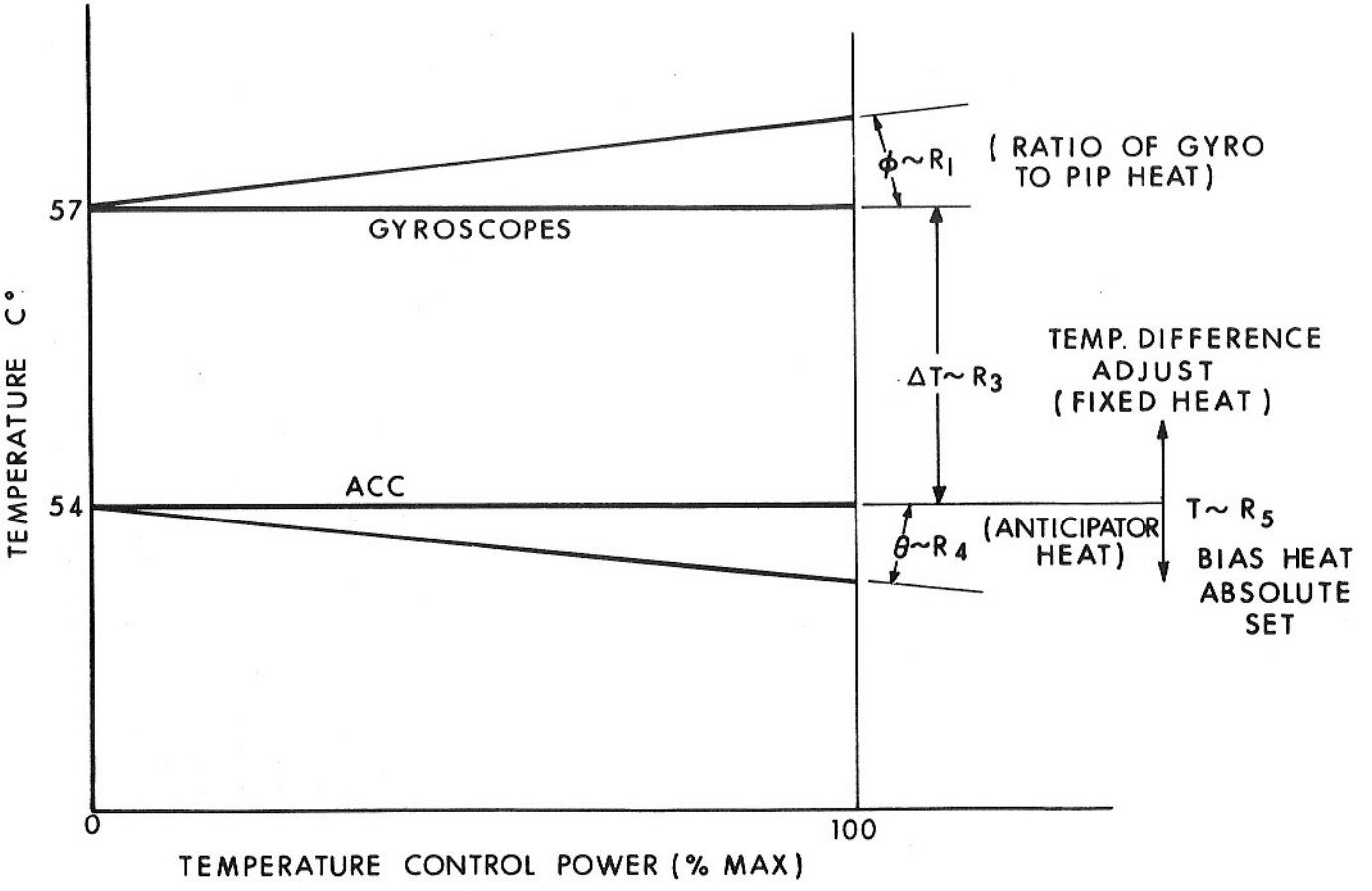

Fig. IV-4 IMU Temperature Control Trimming Resistor Functions

done to reduce uncertainty torques. The thermostat dead zone is 0.17°C. A thermostat heater is used to prevent long delays and to control the limit cycle amplitudes of the inertial components. This heater is the anticipatory heater. Fixed heat is applied to the thermostat to set the absolute temperature of the inertial components.

Mounted on the outer gimbal are a pair of blowers, one on each end of a diameter. These also are thermostatically controlled, their purpose is to increase the dynamic range of the temperature control loop in the presence of environmental disturbances. Each inertial component is held to a constant temperature ± 1/3°C under all environmental temperature and pressure design conditions. The blower control loop is required only under conditions of high environmental conditions or high heat dissipation on the stable member. About 18 watts are dissipated under normal operating conditions on the stable member. The principal portion of this power is in the gyro wheels, about 14 watts. A complete temperature control diagram is shown in Figure IV-3. The principal problems of design have been the reliable control of six inertial instruments with a single thermostat and the design of a precision temperature control system both under accelerating and free fall conditions with wide variations in the environmental disturbances. The temperature difference between IRIGs and PIPs is adjusted by properly proportioning the amount of power in each heater. This balance is obtained by adjustment of R_1. (Refer to Figure IV-3 and IV-4). As the power required to maintain the thermostat in its limit cycle operation is varied (because of environmental or power changes) the temperature error of the IRIGs and PIPs can change proportional to the power required. This proportionality can be adjusted to be either plus or minus, and is adjusted to zero. This results in a zero temperature error, or very nearly so, over the full power range possible. There is a fixed bias heat applied to the PIPs to bring them to their operating temperature under normal conditions. As the PIP temperature deviations are subject to gyro power dissipation, this fixed heat is from the same power supply as the gyro wheels.

The performance of the temperature control system may be seen in Figure IV-5. The thermostat cycle of operation at 50% duty cycle is 0.17°C while at the same time the gyroscope limit cycle has been attenuated to 0.36 millidegrees C° and that of the accelerometers to 5 millidegrees C°. The stable member temperature continues to drop as the control power is increased as one would expect. But the inertial component temperature remains constant throughout the power range. The blower extends the dynamic range of operation, is used infrequently and is limit cycled by a thermostat. There is a separate sensor to detect temperature out of limits to caution the astronaut should this occur. In addition, high limit mechanical thermostats are used in every heater power line

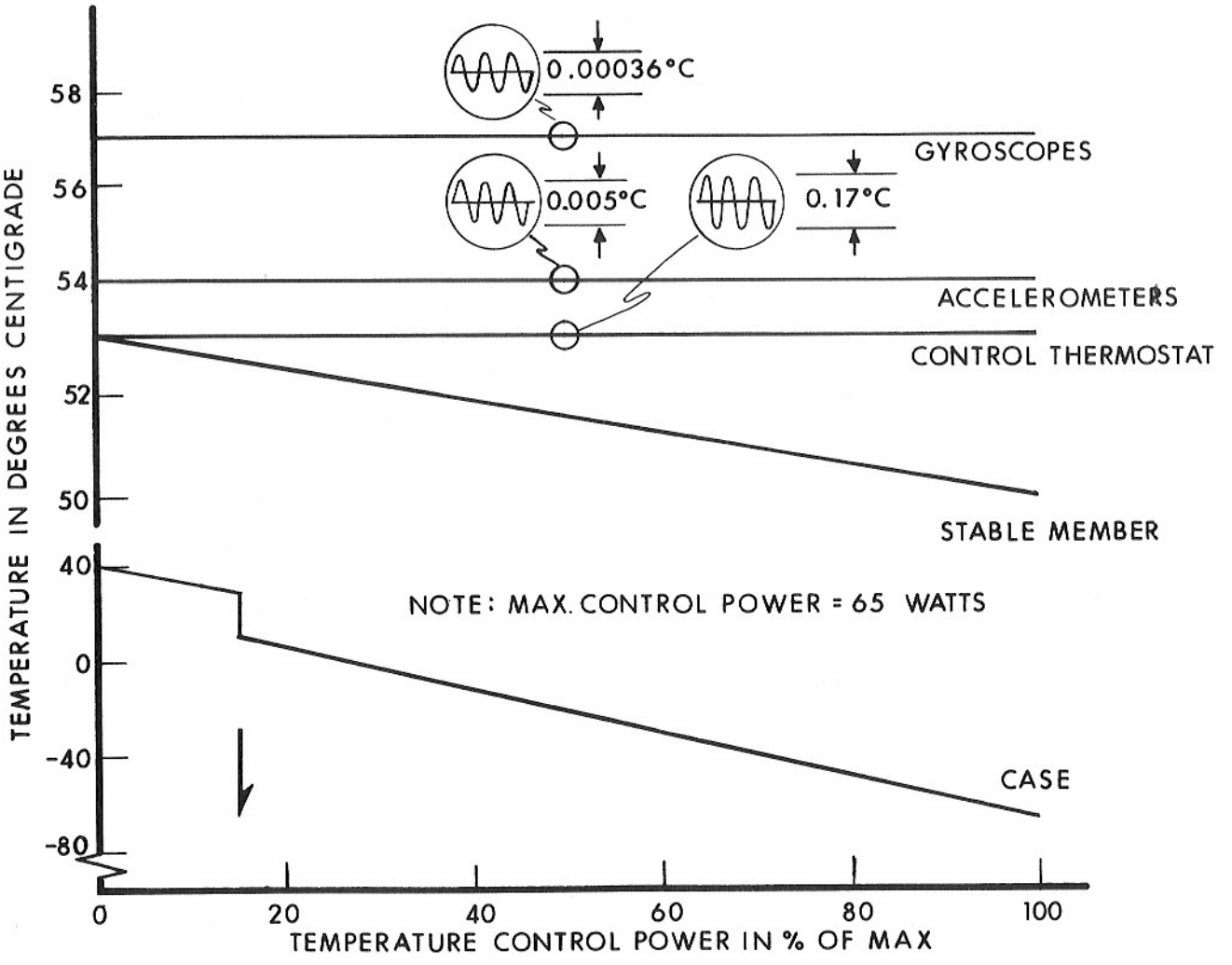

Fig. IV-5 IMU Temperature Profile vs Temperature Control Power

to prevent an over heated condition. These are set to open the heater power at a temperature of about 5°C over the normal control temperature. These have been rarely used but when necessary have prevented damage to valuable equipment.*

The GSE (Ground Support Equipment) heaters and sensors have been provided for ground handling. The IMU once assembled is maintained at temperature. This necessitates times and places of operation where normal power may not be available. Separate heaters and sensors are provided isolated from airborne control. Thus it is possible with the system in the spacecraft to be maintained at temperature with a portable temperature controller with normal power off or on.

Vibration - Before proceeding into the vibration environment it is well to discuss some of the mechanical construction features. The stable member itself is a sintered block of beryllium with drilled holes for each inertial component. These inertial components are pre-aligned in a test stand and assembled into the stable member in an aligned condition. This saves considerable adjustment of alignment at later stages of testing. A pre-wired harness with connectors is laid on to the stable member and interconnection is made. At each end of the stable member are intergimbal assemblies. These house the slip rings to electrically interconnect rotating members. The slip rings are 40 or 50 circuit elements depending upon axis location, the larger number required at the middle and outer axis. Much effort has gone into the design of reliable rotary slip rings which will give unlimited angular freedom of motion. There is a double pair of brushes for each circuit spaced 0.025 inches apart. Each circuit with two feet of #30 AWG has less than 1/3 of an ohm resistance. Electrical coupling does take place between adjacent circuits. Coupling is approximately inversely proportional to the spacing between circuits. With proper selection of circuit placement on the slip ring cross coupling effects can be reduced to negligible amounts. Each contact is rated for 2 amps of current. Only heater power utilizes this much current while everything else is less than 1 amp. High current carrying load slip rings are paralleled for reliability reasons. Early design considerations allow for about 10% spares. As the design progresses toward maturity these spares are usually reduced and finally all utilized for redundancy.

The gimbal construction is spherical. Gimbals are interconnected by means of an intergimbal assembly which contains the resolvers, dc gimbal torque motors, slip rings, stub shaft and a duplex pair of preloaded bearings. Surrounding the stable member is the middle gimbal, and surrounding the middle gimbal is the outer gimbal which is next to the case. The intergimbal assemblies contain either a resolver or a dc torque motor. Each axis utilizes one dc torque motor and a single resolver which is both a single speed resolver and a sixteen speed resolver utilizing the same excitation winding. In addition, on the inner axis is a

*This work done by Edward S. Hickey, MIT Instrumentation Laboratory

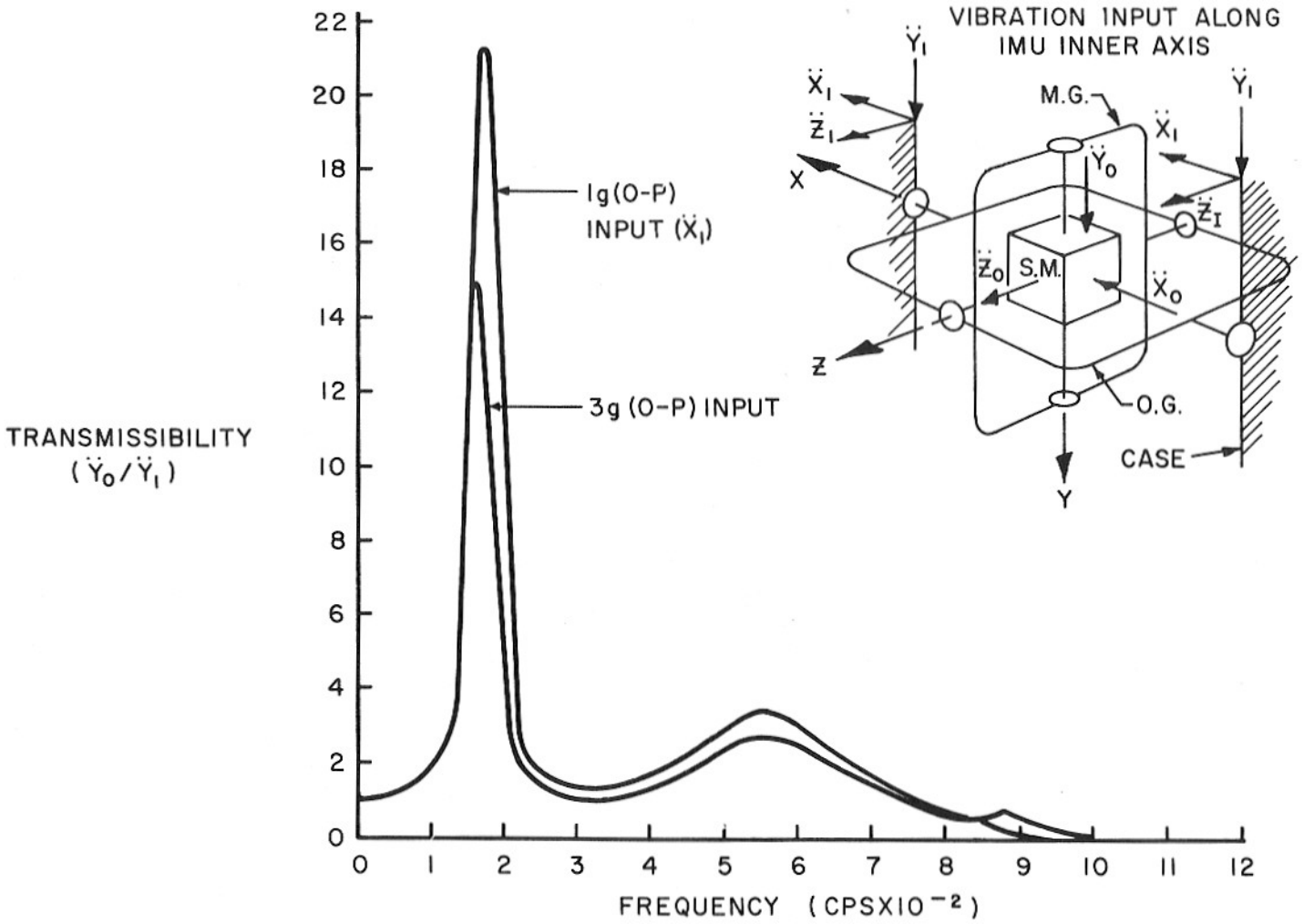

Fig. IV-6 Apollo IMU-VM (12.5) Vibration Test Results
Stable Member Response Curves

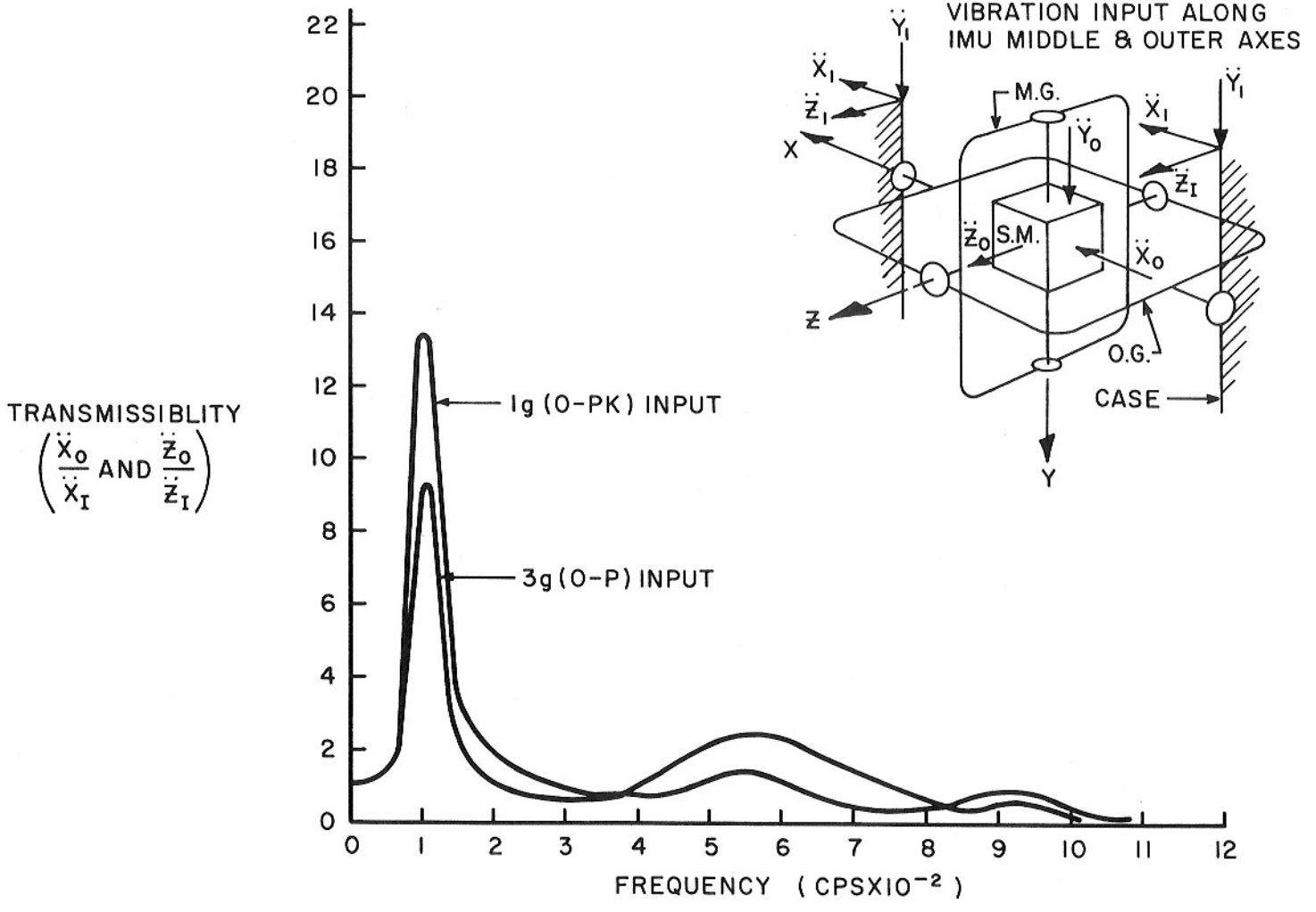

Fig. IV-7 Apollo IMU-VM (12.5) Vibration Test Results
Stable Member Response Curves

gyro error resolver to resolve X and Z gyro error voltages by the angle of the inner gimbal. Each axis has a duplex pair of preloaded bearings. These inter-gimbal assemblies are again made of beryllium for the housing and stub shaft in order to decrease weight.

The IMU, as a mechanical element, forms a system of masses, springs, and dampers, with non-linear behavior. As a complex mechanical system it will resonate at certain frequencies. The lowest frequency resonant vibration ratio of the amplitude of the stable member to that of the input to the case is the greatest. This ratio, called transmissibility, is non-linear in that the ratio decreases with increasing input amplitudes. The elements must be structurally sound enough to withstand the flight environment. Shown in Figures IV-6 and IV-7 is the transmissibility of the IMU. The expected flight environment is less 0.044 g^2/cps. Each IMU is given a workmanship vibration test from 20 to 2,000 cps at least 1 g rms input along each axis.

The resonant peaks may be reduced by adding vibration dampers along each axis which provide a Coulomb friction force for motion along the axis but which do not change the friction torque about the axis.

Gyroscopes and Stabilization - The gyroscopes used are single-degree-of-freedom integrating gyroscopes of a type previously described.[1] The angular momentum is $\frac{10^6}{2}$ gm cm^2/sec developed by a wheel support by a pair of preloaded ball bearings with a 3 lb preload. This wheel has a hysteresis ring on it with a motor stator surrounding it on the inside of a spherical float. The float is a beryllium member again designed to yield the highest ratio of wheel to float weight. Flexible power leads carry power from the case to float. These power leads create less than 1/2 dyne cm of torque on the float. The fluid used for buoyant support is a brominated fluorocarbon with a density of 2.385 gms/CC at 58°C. The fluid is fractionally distilled to yield polymers of approximately the same length and nearly the same viscosity. This prevents fluid stratification under operating and storage conditions. The damping about the output axis is $4.6 \cdot 10^5$ dyne cm/radian/sec. In addition, to the fluid support there is an electromagnetic suspension system to provide both axial and radial suspension of the float with respect to the case. Such suspension systems have been previously described.[2]

The axis definition for the instrument has previously been described. Shown in Figure IV-9 is the signal generator which develops a voltage modulated by the angle of the float with respect to the case, A_{c-f}. This is the rotation of the stable member about the gyro non-rotating input axis. There is with each gyroscope a set of prealignment hardware. This provides integrally with each prealigned instrument the following items:

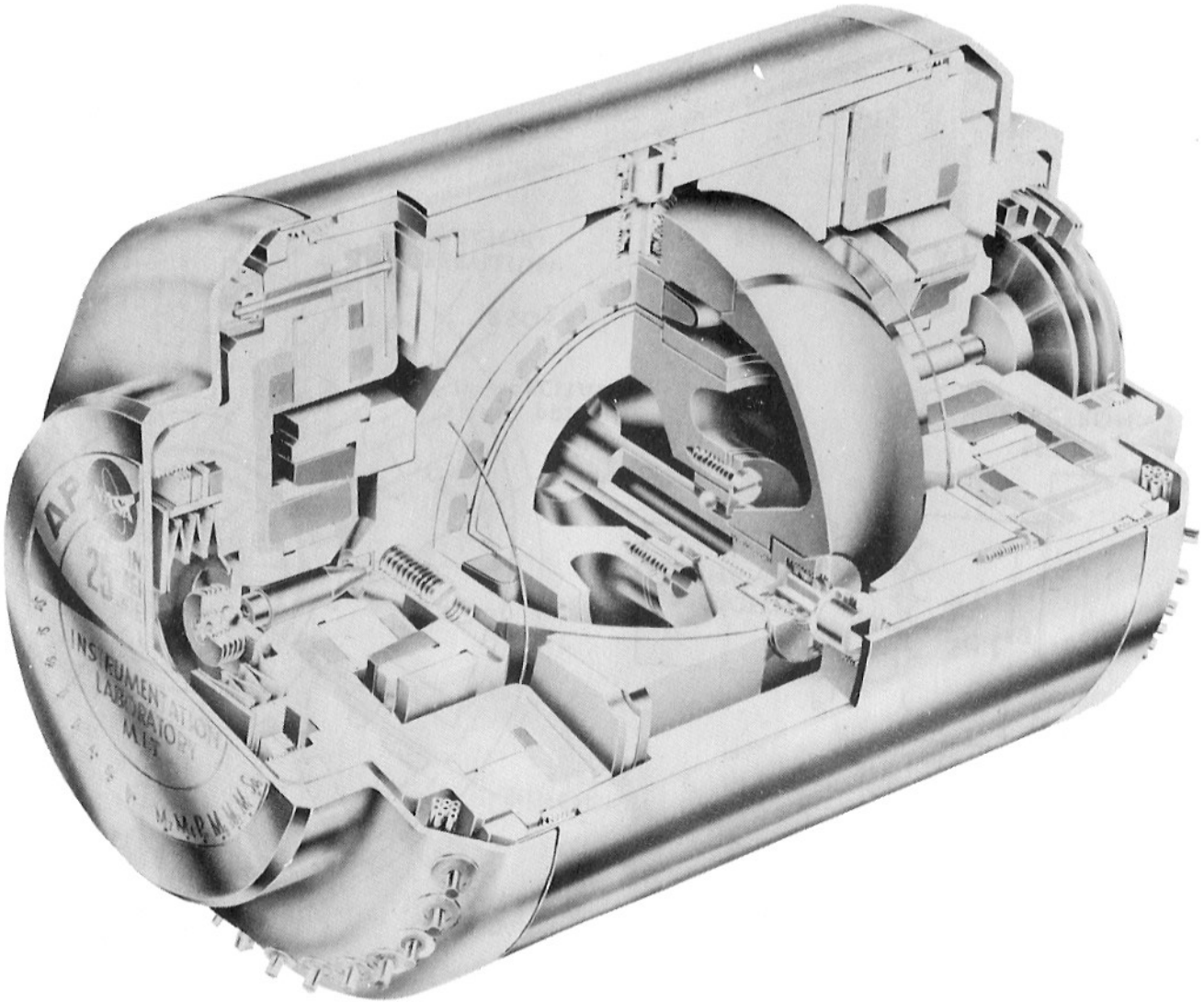

Fig. IV-8 Apollo II IRIG

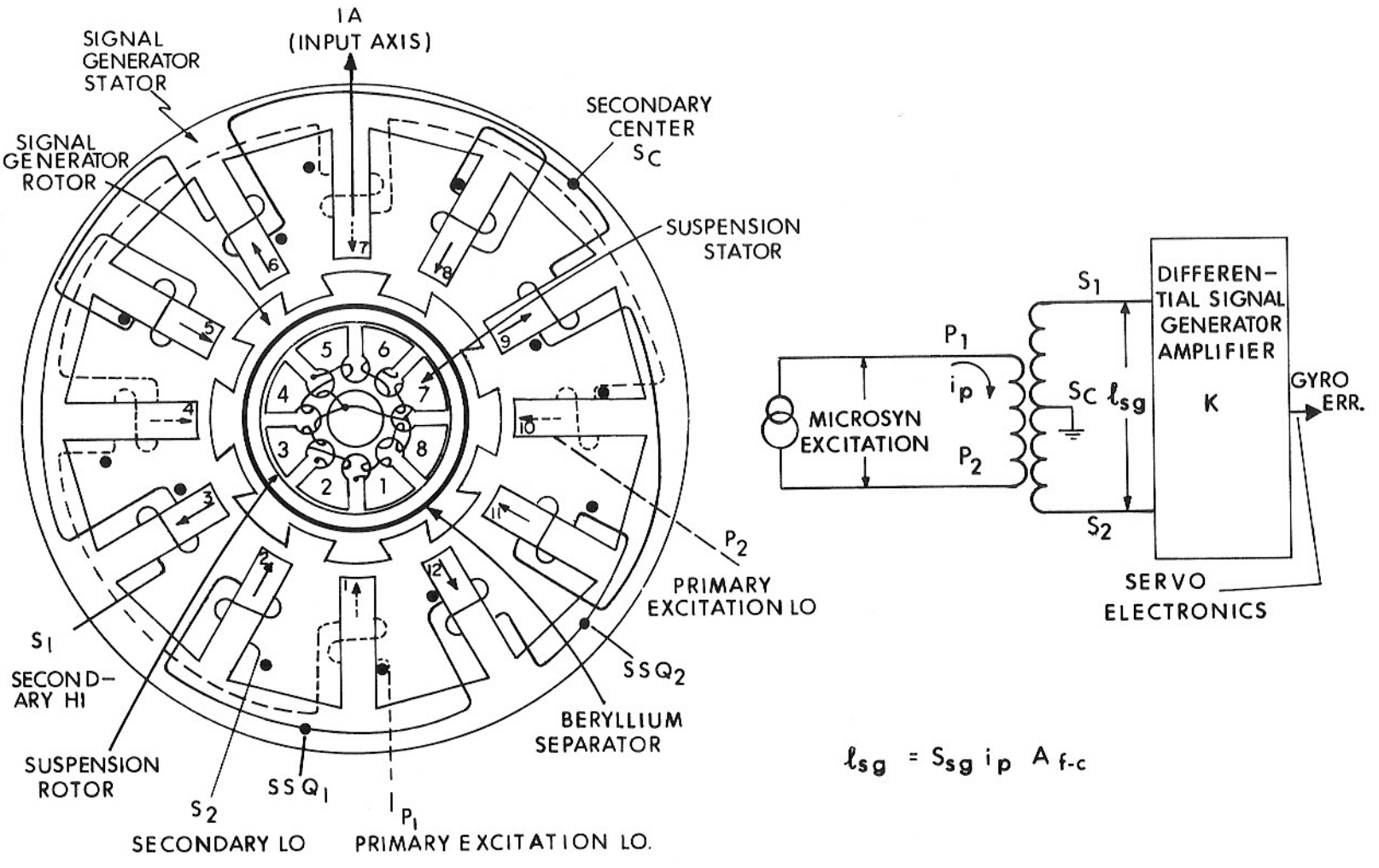

Fig. IV-9 Apollo II IRIG Signal and Suspension Microsyn

A. Suspension Capacitors for Microsyn Suspension
B. Temperature Sensor Normalization
C. End Mount Heater Pre-aligned to Gyro IA.
D. Torque Generator Normalization
E. Signal Generator Preamplifier with normalized gain

The gyro is prealigned on a test stand with the input axis aligned about the output axis relative to a slot in the mounting ring. The alignment is carried over to the stable member where a pin is precisely located to pick up the slot.

The use of prealigned components has made assembly techniques simpler and has brought about excellent correlation between component and system performance of the gyroscope. Deviations in performance between component and system are less than 10 meru (milliearth rate unit). 1 meru = 0.015 degrees per hour.

Each gimbal axis contains a dc torque motor used to null the deviations of the gyro input axis with respect to the case. These direct drive motors have been designed with sensitivities of 1.12 ft lbs/amp. The gyro error signals are fed to the gimbal servo amplifier which with its proper dynamic compensation are used to stabilize the inner member. The performance of the gimbal servos is best described by their ability to attenuate angular deviations of the stable member in the presence of torque disturbances. Shown in Figure IV-10 is the performance of each axis of the IMU gimbal servo. Among the design problems are the mode switching from coarse align (resolver control) to fine align (gyro control), synchronization from turn-on or switch over conditions, performance under power supply changes, gain changes from geometrical variations, and torque disturbances.

Gyro torquing is required for precision alignment of the stable member at prelaunch and for in-flight alignment. The fine alignment procedure and mechanization has previously been described. The gyroscope has a torque generator used in a digital torque command loop. This loop accepts commands from the computer by a pulse train with equal pulse width spacing. The torque commanded is a constant magnitude and modulated only by the time interval. The computer could thus command one equivalent pulse incremental angle ($2\pi / 2^{21}$ radians/pulse). One precision current switch is used for all three gyroscopes and the commands are multiplexed in one selector network. The torque level control will be described later. (See Chapter IV-2) The torque generator is normalized in gain to command a fixed angular velocity for a fixed current. This digital angle command from the computer to the IMU permits the stable member to be oriented within the uncertainty of the angle read system ($\Delta\theta$ = 40 arc sec). It furthermore, has the advantage of no current applied to the gyro during periods other than alignment. The gyroscopes are oriented on the stable member with Y and Z gyro output axis along

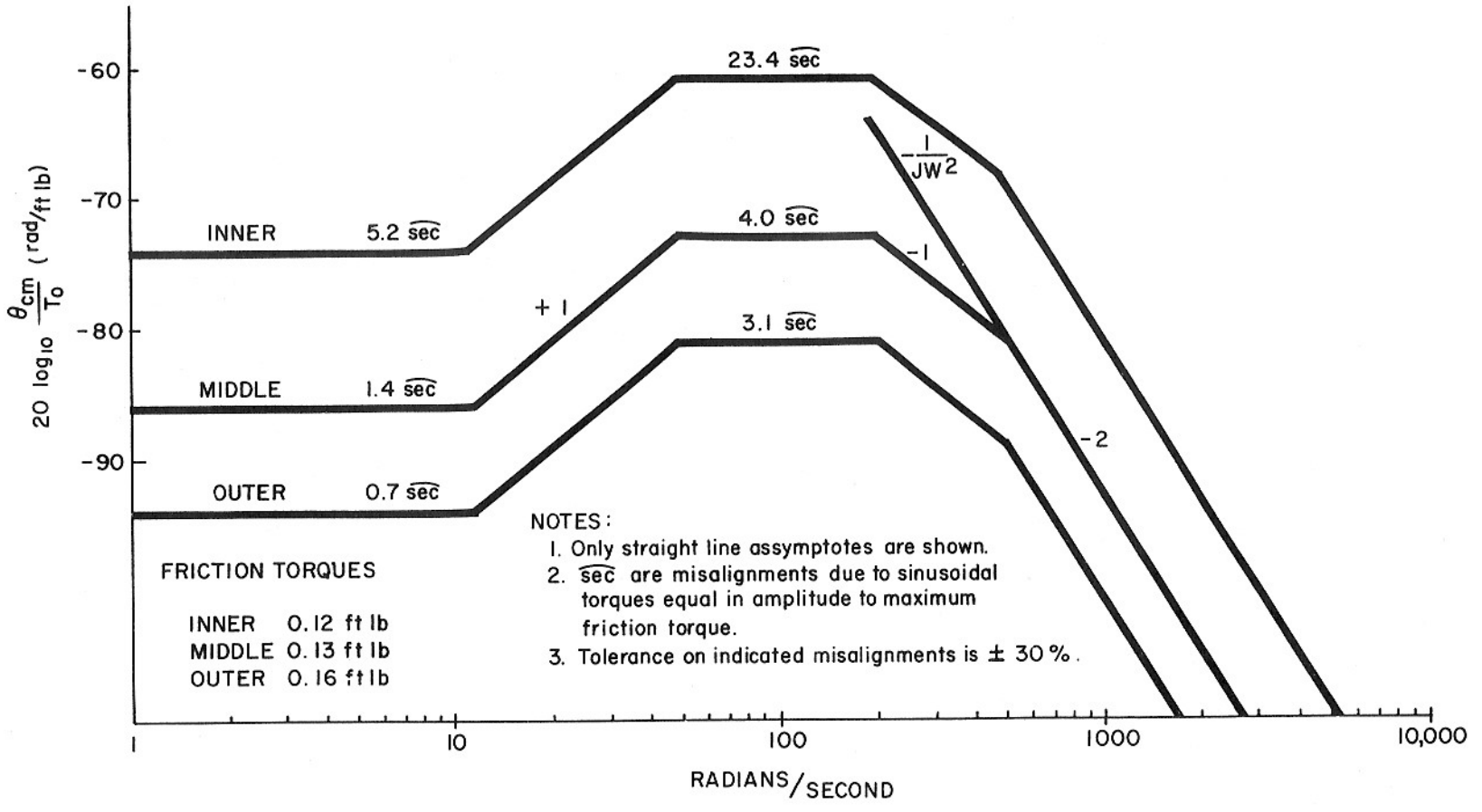

Fig. IV-10 Inertial Platform Misalignment Due to Friction Torques vs Frequency

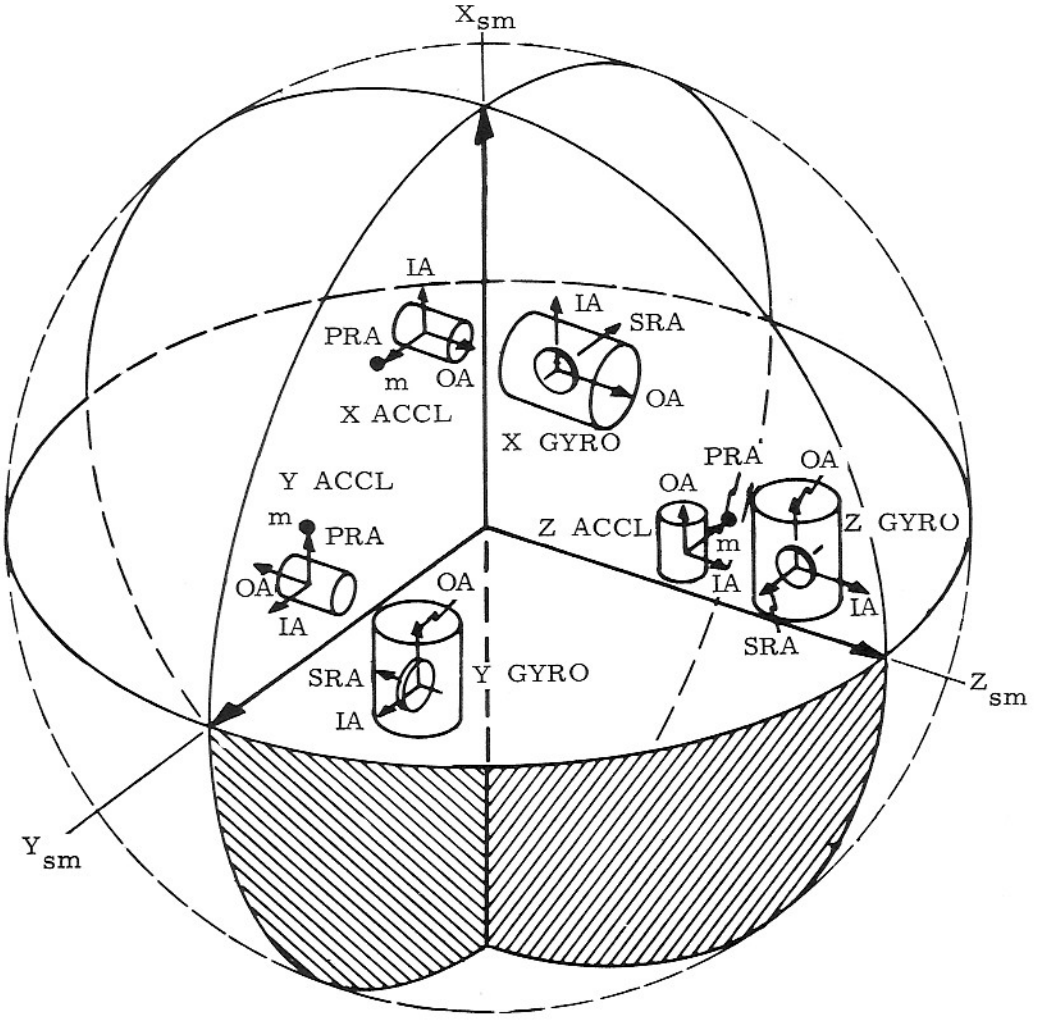

Fig. IV-11 Stable Member Geometry

ΔV = 10,220 ft/sec

MAX ACCELERATION 40 ft/sec^2

PA = -101.87°

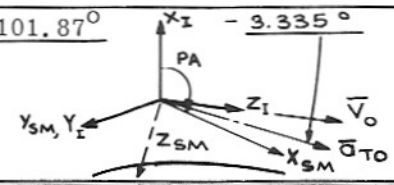

				Error Coefficient	Final Position Error in Target Axes in feet			Final Velocity Error in Target Axes in ft/sec		
					Alt.	Track	Range	Alt.	Track	Range
STABLE Member	Initial S. M. Alignment Errors	$A_{(SM)XI}$		0.2 mr		99			0.82	
		$A_{(SM)YI}$		0.2 mr	277		-77	2.09		-0.46
		$A_{(SM)ZI}$		0.2 mr		-261			-1.86	
ACCELEROMETER	Accel. IA Non-orthogonality	X to Y		0.10 mr						
		X to Z		0.10 mr	-1		-6	-0.0002		0.0008
		Y to Z		0.10 mr						
	Bias Error	ACBX		0.2 cm/sec^2	-70		-305	-0.46		-1.94
		ACBY		0.2 cm/sec^2		-313			-1.99	
		ACBZ		0.2 cm/sec^2	316		-72	2.08		-0.46
	Scale Factor Error	SFEX		100 PPM	-31		-136	-0.23		-0.99
		SFEY		100 PPM		0			0	
		SFEZ		100 PPM	-7		2	-0.004		0.0004
	Accel. Sq. Sensitive Indication Error	NCXX		$10\mu g/g^2$	-3		-13	-0.08		-0.11
		NCYY		$10\mu g/g^2$		0			0	
		NCZZ		$10\mu g/g^2$	0.08		-0.02	0.0006		-0.0001
GYRO	Bias Drift Drift Time before Traj start: 15 min. (Init Mlm. = 0.33 mr. for 5 meru drift)	BDX	Direct effect	5 meru		0.4			-0.03	
			Eff on Init Mlm			163.1			1.35	
			Combined eff			163.5			1.32	
		BDY	Direct effect	5 meru	59		-14	0.66		-0.12
			Eff on Init Mlm		454		-126	3.44		-0.76
			Combined eff		513		-140	4.10		-0.88
		BDZ	Direct effect	5 meru		59			0.65	
			Eff on Init Mlm			-428			-3.05	
			Combined eff			-369			-2.40	
	Acceleration Sensitive Drift	ADIAX		15 meru/g^2		0.3			-0.08	
		ADSRAY		10 meru/g^2	7		-2	0.05		-0.012
		ADIAZ		15 meru/g^2		-11			-0.08	
	Acceleration Squared Sensitive Drift	$A^2D_{(IA)(IA)X}$		1 meru/g^2		-0.03			-0.006	
		$A^2D_{(SRA)(SRA)Y}$		1 meru/g^2	0.07		-0.02	0.0007		-0.0001
		$A^2D_{(IA)(IA)Z}$		1 meru/g^2		0.07			0.0006	

Fig. IV-12 Translunar Injection Trajectory Cutoff Coefficients

(V_0 = 36,200 ft/sec., γ_o = - 6.0 deg., Max. G = 5.45, Platf.Angle = -35.7°)

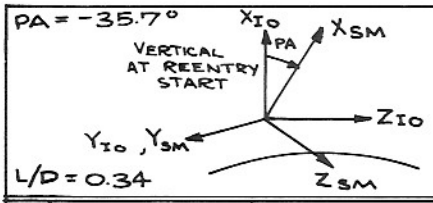

				Error Coefficient	Final Position Error in Target Axes in feet		
					Alt.	Track	Range
STABLE Member	Initial S.M. Alignment Errors (Uncorrelated)	$A_{(SM)XI}$		0.2 mr	130	946	28
		$A_{(SM)YI}$		0.2 mr	-2,360	-6	376
		$A_{(SM)ZI}$		0.2 mr	-44	1,796	101
ACCELEROMETER	Accel. IA Non-orthogonalty	X to Y		0.1 mr			
		X to Z		0.1 mr	-1,172	-3	23
		Y to Z		0.1 mr			
	Bias Error	ACBX		0.2 cm/sec^2	-1,593	-4	32
		ACBY		0.2 cm/sec^2	-4	-1,361	0
		ACBZ		0.2 cm/sec^2	35	0	-1,369
	Scale Factor Error	SFEX		100 PPM	215	1	-8
		SFEY		100 PPM	0	-52	0
		SFEZ		100 PPM	-26	0	1,007
	Accel. Sq. Sensitive Indication Error	NCXX		10μg/g^2	-49	0	1
		NCYY		10μg/g^2	0	-20	0
		NCZZ		10μg/g^2	7	0	-281
GYRO	Bias Drift Drift Time before Traj. start: 45 min. (Init. Mlm. = 0.98 mr. for 5 meru drift)	BDX	Direct effect	5 meru	1	852	7
			Eff on Init Mlm		641	4,655	139
			Combined eff		642	5,507	146
		BDY	Direct effect	5 meru	-937	-1	-9
			Eff on Init Mlm		-11,618	-28	1,850
			Combined eff		-12,555	-29	1,841
		BDZ	Direct effect	5 meru	-11	19	1
			Eff on Init Mlm		-217	8,840	499
			Combined eff		-228	8,859	500
	Acceleration Sensitive Drift	ADIAX		15 meru/g	-1	-879	10
		ADSRAY		10 meru/g	-2,832	-4	9
		ADIAZ		15 meru/g	17	-33	-3
	Acceleration Squared Sensitive Drift	$A^2_{D(IA)(IA)X}$		1 meru/g^2	0	113	0
		$A^2_{D(SRA)(SRA)Y}$		1 meru/g^2	-808	-1	13
		$A^2_{D(IA)(IA)Z}$		1 meru/g^2	-8	-3	1

Fig. IV-13 2,000 N. Mile Earth Reentry Trajectory Errors

X_{sm}. This axis is usually aligned along the thrust axis. This inertial component orientation reduces the acceleration sensitive torques in the gyros. The Y_{sm} axis is usually aligned such that it is normal to the plane of maneuver. For this reason the X gyro SRA is along Y_{sm} as can be seen in Figure IV-11. For the same reason the Z SRA axis is along Y_{sm}.

The largest error contributors per unit of error following any maneuver are the premaneuver errors. That is to say that the effects of gyro drift during thrusting create less error uncertainty in position and velocity at the end of thrust period than those misalignments due to drift between alignment and start of thrust. The error in free fall from the time of alignment to the start of any acceleration maneuver is time dependent upon the gyro non-acceleration sensitive drift (bias drift). As an example the ratio of error created by 1 meru of drift for 15 minutes prior to the start of translunar injection to that error created by the same drift during thrusting is approximately 400:1. A table of error coefficients for two thrusting maneuvers are shown in Figure IV-12, and Figure IV-13. This same fact is readily apparent. Every effort has been made to reduce gyro bias drift uncertainty and magnitude.

The torque generator has been designed to be dc torqued with low residual magnetism uncertainty torques. It is a twelve pole stator with an eight pole rotor creating 4500 dyne cm of torque with a current excitation of 0.1 amps. The beryllium separator prevents the use of the microsyn excitation as a reset coil or degausser for the rotor. Dipole storage in the rotor and stator would create residual torque in the gyro and this torque magnitude and sign would be a function of its past history. It would be possible to return the state of the magnetic material to its original condition in most cases by appropriate commands from the computer. However, the use of a reset coil with ac excitation from the microsyn excitation voltage supply serves to keep the state of the magnetic material constant following any pulse torque commands from the computer. There is a winding around each set of three poles which acts as a reset winding for both rotor and stator. Further use of this reset winding may be made if one recognizes that if the flux through one stator pole were unbalanced there would be a torque created on the float. The bias compensation winding on pole nine is used to create a torque equal and opposite to all the non-gravity sensitive torques and thus reduce the bias drift to zero. The torques creating bias drift come from two sources: flex leads, and microsyns. The microsyn torques are proportional to the microsyn excitation voltage squared. The bias compensation winding torque changes due to excitation voltage changes are exactly equal and of negative polarity relative to the microsyn torque changes from the same source. Only the flex lead torque magnitude may be compensated by the bias winding.

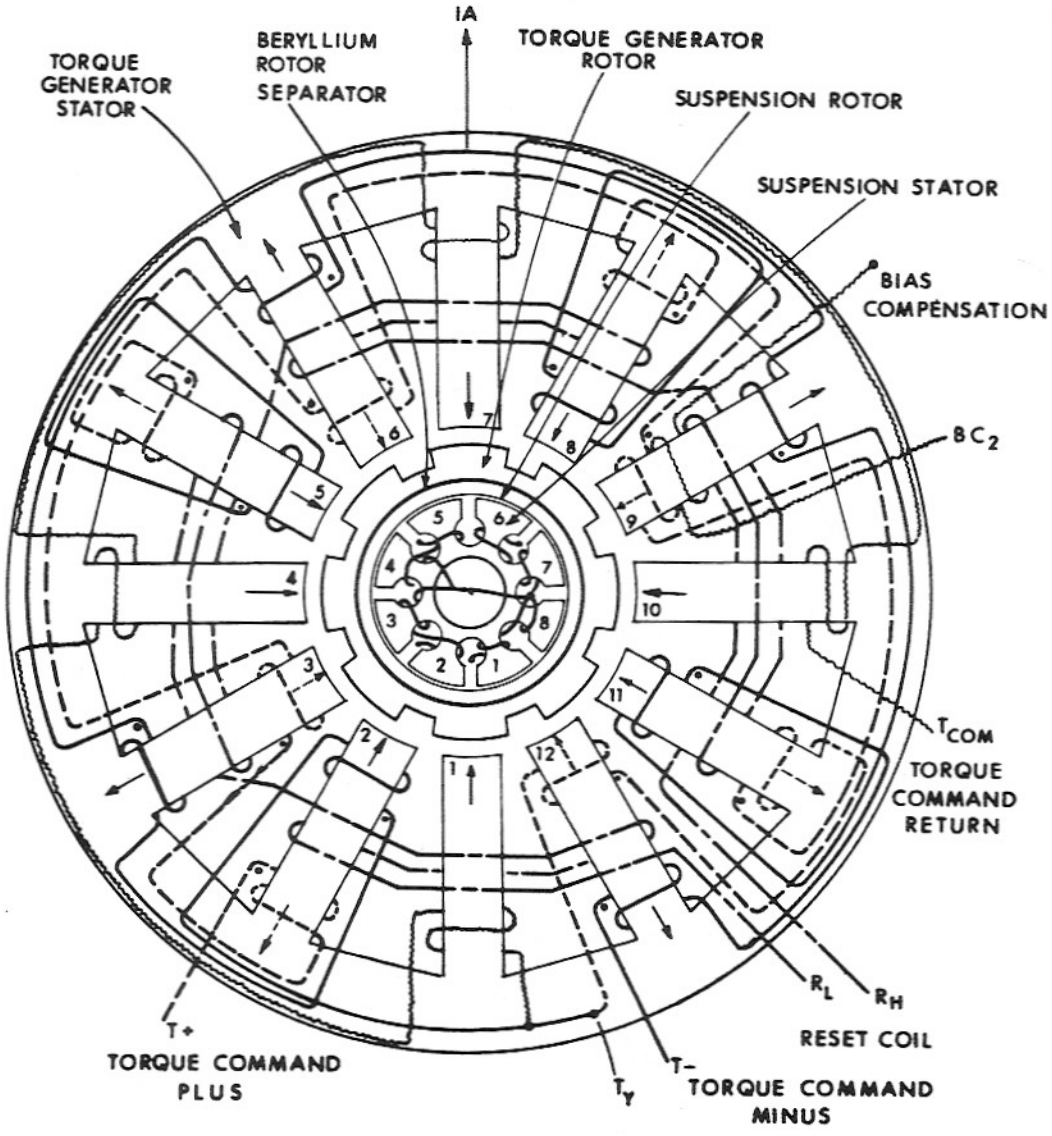

Fig. IV-14 Apollo II Torque Generator and Suspension

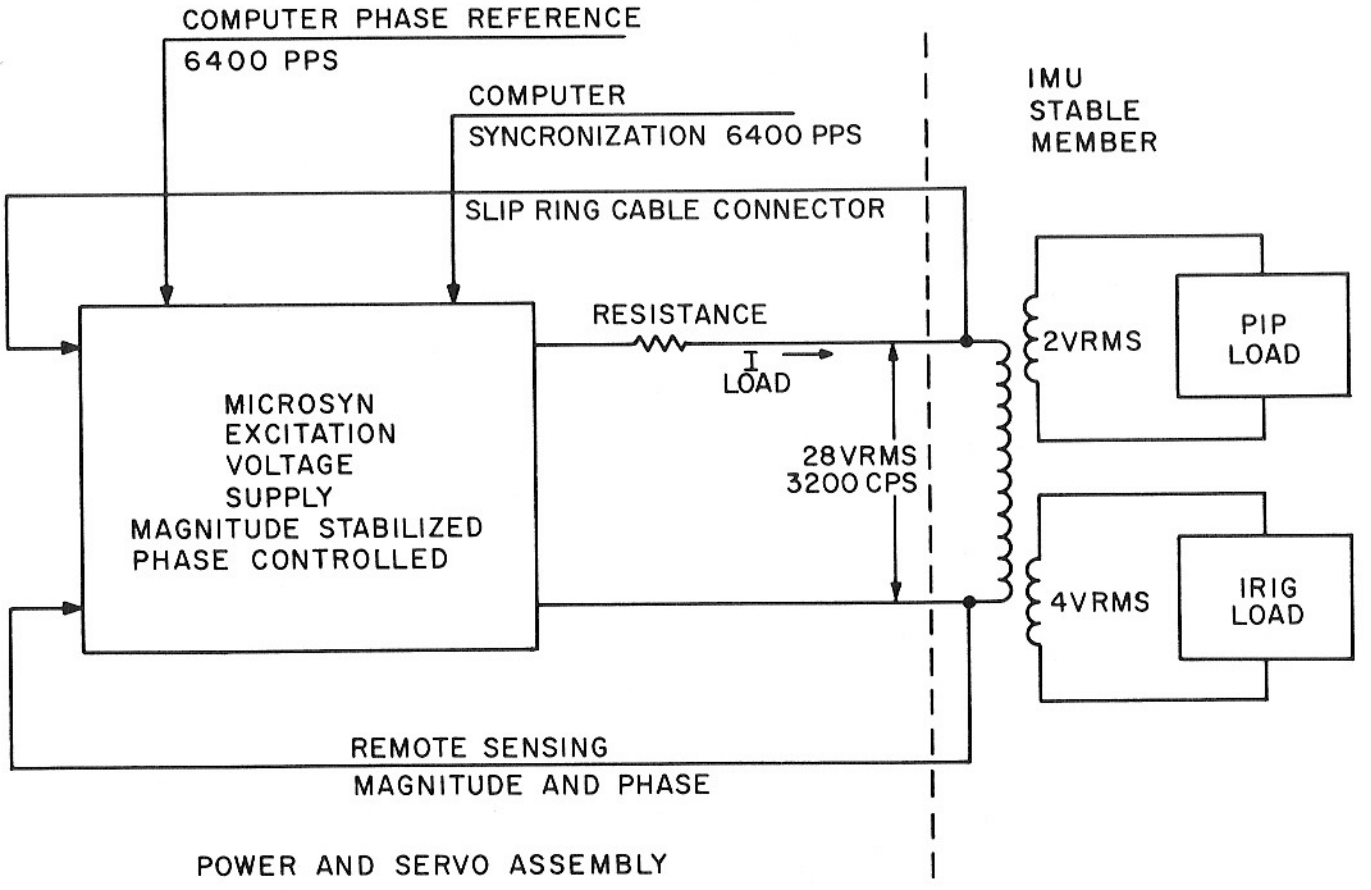

Fig. IV-15 Microsyn Excitation Voltage Supply

The microsyn excitation for both gyros and accelerometers is from a single source located in the power and servo assembly, PSA. The voltage level on the IMU stable member is stable to within 1% of the value required (2 volts for the PIPs and 4 volts for the IRIGs) under the design disturbance conditions. The magnitude and phase of the voltage on the stable member is controlled. All ac power supplies are synchronized to the guidance computer clock. Also dc to dc converter or dc supplies using multivibrators as ac sources for rectification are also synchronized to the computer. The method of synchronization is to use a multivibrator which will free run at a lower frequency without the computer pulses. This will assure operation of the IMU power supplier in the event of a computer failure. With the computer pulses these supplies will be synchronized. In addition, the microsyn excitation supply voltage is phase locked to the computer. The voltage stability and phase stability is required at the inertial component. For power transmission there is a step down transformer on the stable member. This reduces the slip ring current and the voltage drop effects due to slip ring, cable and connector resistance. The stable member voltage is sensed at the primary transformer side and compared to a voltage and phase reference. Phase is controlled to within $\pm$ $1/2^{o}$ of the computer reference. On the stable member each PIP has the same length of wire from the transformer to the PIP input terminals on the instrument.

CHAPTER IV-2

THE PULSED INTEGRATING PENDULOUS ACCELEROMETER (PIPA)

Basic Operation - The PIPA block diagram is shown in Figure IV-16. The inertial sensor is a single-degree-of-freedom pendulum with a pendulosity of 1/4 gm cm. The pendulum is mounted on the stable member and is non-rotating with respect to inertial space. The signal generator is a variable reluctance device termed a signal generator microsyn. It is excited from a sinusoidal source which is synchronized and phase locked to the guidance computer. The signal generator output is voltage modulated by the angle of the pendulum float with respect to case (A_{c-f}) and the float angular velocity ($\dot{A}_{c-f}$). The voltage may be considered to contain only float angle information. This signal, amplified, is used in an interrogator. The interrogator is a peak detecting device used to determine sign and magnitude of the float angle at discrete times. These discrete times are the computer clock times (ΔT) synchronized with sinusoidal excitation. Only float angle sign is determined and the operation is binary. The interrogator output is a command to torque the float angle to null. The current switch directs a constant current source into either the odd poles or even poles of an eight pole torque microsyn. The torque generator creates a torque either positive or negative proportional to the square of the current in the windings. Current is controlled constant by comparison of a precision voltage reference with the voltage drop across a precision resistor in the current loop.

Dynamic Operation - The basic loop equation is neglecting uncertainty torques about the output axis and making the small angle assumption: $\cos A_{c-f} = 1$, $\sin A_{c-1} = A_{c-f}$.

$$J \ddot{A}_{I-f} + C \dot{A}_{c-f} = M_{tg} + ml\, a_{IA} \qquad \text{(IV-1)}$$

Where

J = Float Inertia

C = Damping about the output axis

A_{c-f} = Float angle with respect to the case (c-f)

A_{I-f} = Float angle with respect to Inertial Space

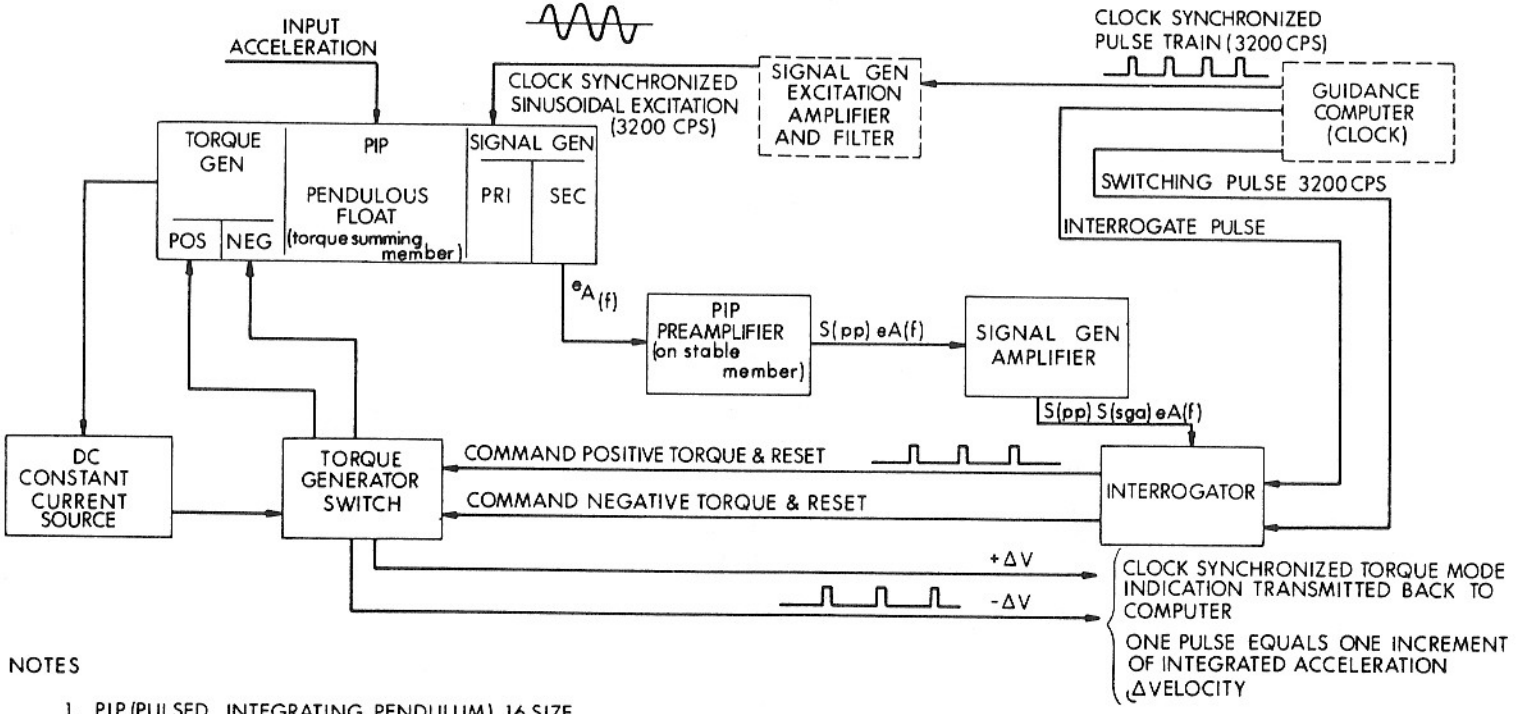

NOTES

1. PIP (PULSED INTEGRATING PENDULUM) 16 SIZE SINGLE DEGREE OF FREEDOM PENDULOUS UNIT
2. WAVE FORMS SHOW CONDITION FOR NEGATIVE INPUT ACCELERATION OF PIP CASE

ΔV COMMAND MODULE 5.85 CM/SEC/PULSE

ΔV LEM 1.0 CM/SEC/PULSE

Fig. IV-16 PIP Accelerometer Block Diagram

M_{tg} = Torque generator torque

a_{IA} = Acceleration along the input axis

$$V_{IA} = \int_o^t a_{IA}\, dt$$

Integrating yields

$$J\,\dot{A}_{I-f} + C\,A_{c-f} + \text{Initial conditions} = \int_o^t M_{tg}\, dt + ml \int_o^t a_{IA}\, dt$$

Considering the float storage and initial conditions for the accelerometer as an error (velocity stored, V_s)

$$V_s = \int_o^t M_{tg}\, dt + ml\, V_{IA}$$

$$ml\, V_{IA} - V_s = - \int_o^t M_{tg}\, dt \qquad \text{(IV-2)}$$

Since M_{tg} is controlled to be constant and permitted to change sign only at discrete times (ΔT) the integral may be replaced by summation:

$$ml\, V_{IA} - V_s = - \sum_{o}^{n+p} M_{tg}\, \Delta T = \Delta T\, M_{tg}\, (n - p) \qquad \text{(IV-3)}$$

where n = number of negative torque commands

p = number of positive torque commands

Neglecting for the moment V_s

$$V_{IA} = \frac{M_{tg}}{ml}\, \Delta T\, (n - p) \qquad \text{(IV-4)}$$

The accelerometer scale factor (SF) is then $\frac{M_{tg}\, \Delta T}{ml}$ per pulse and the integrated acceleration or velocity increment per pulse is the scale factor. The net velocity is the net number of minus and plus torque commands, (n - p) sign considered, times the scale factor.

The torque is constantly applied and only switched in direction. The system then behaves as a relay system with a delay due to sampling but no hysteresis. The system limit cycles and the limit cycle behavior is of importance near zero input acceleration as the stored velocity is a function of the magnitude of the limit cycle. The dynamic behavior may be described by collecting together all linear elements (the pendulum, amplifiers, signal generators, etc) as G (s) and the switching of torque as a relay either at + 1 or - 1 together with the sampler as N (s). (See Figure IV-19)

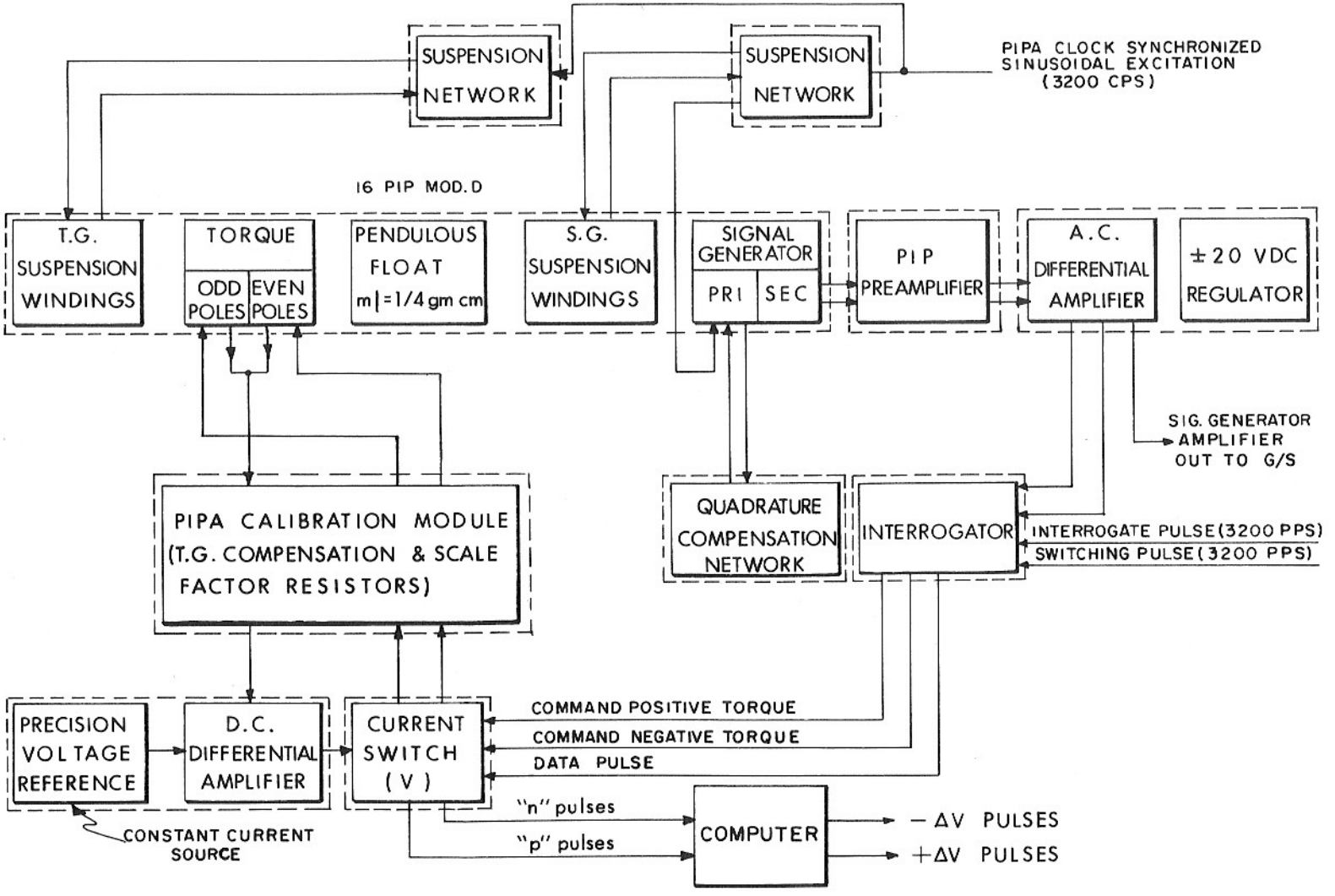

Fig. IV-17 PIP Accelerometer Module Block Diagram

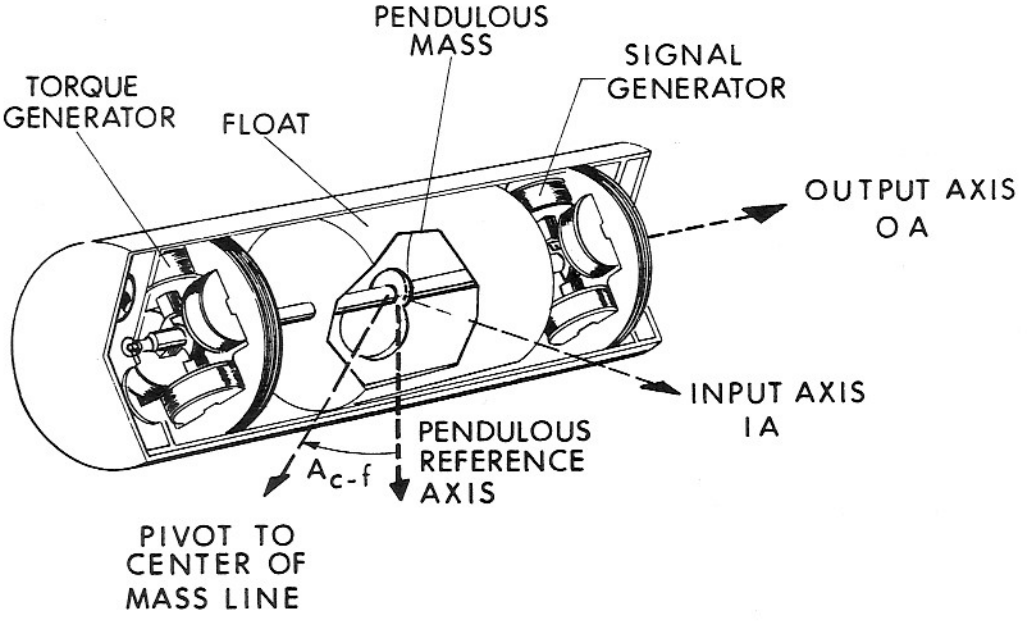

Fig. IV-18 Pulsed Integrating Pendulum Schematic

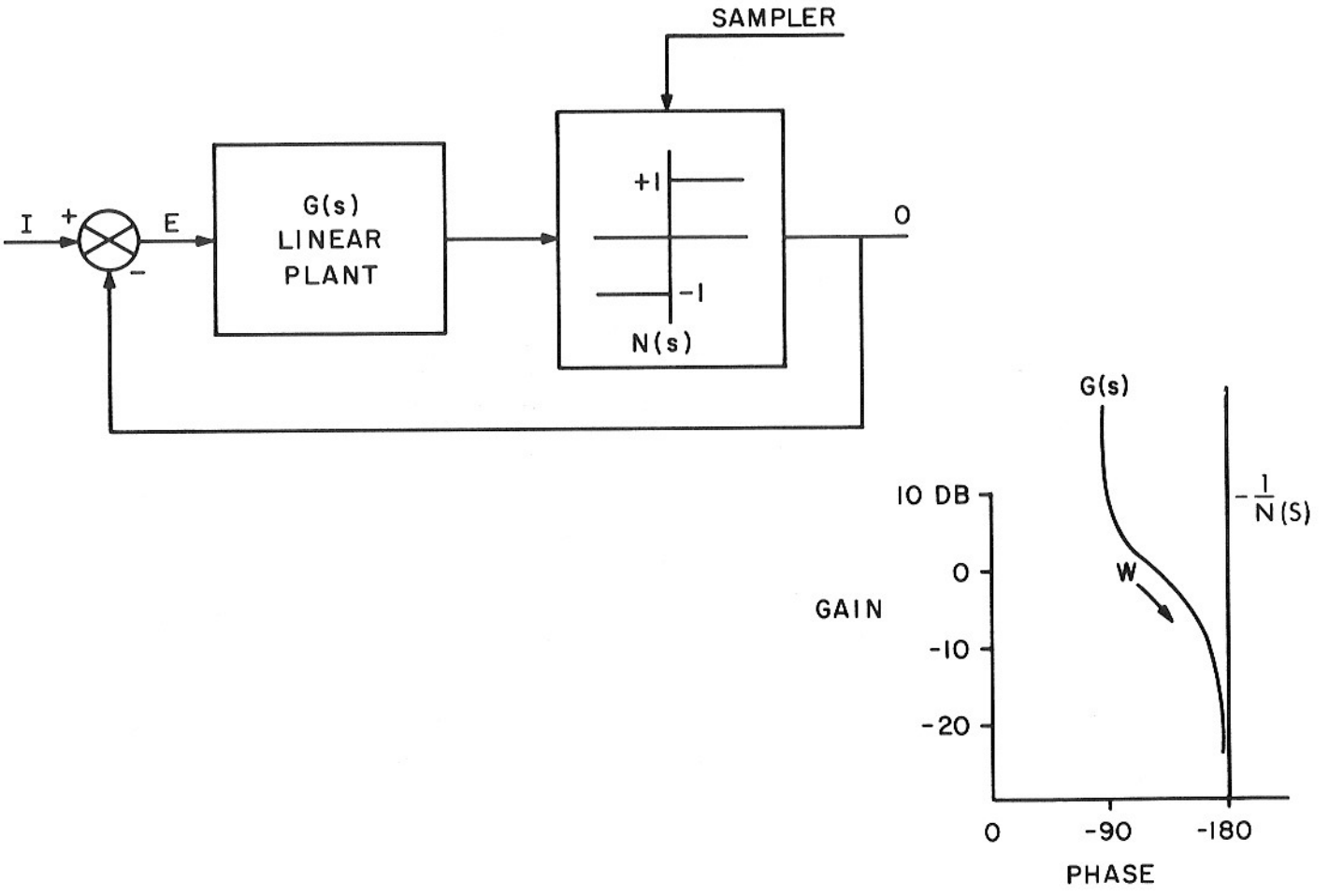

Fig. IV-19 Relay Control System

$$\frac{O}{I} = \frac{G(s)\ N(s)}{1 + G(s)\ N(s)}$$

This loop will oscillate when

$$1 + G(s)\ N(s) = O$$

or

$$G(s) = -\frac{1}{N(s)}$$

Consider for an example only the dynamics of the inertial component as the linear plant.

$$G(s) = \frac{K}{s\left(1 + \frac{Js}{G}\right)} \qquad \text{(IV-6)}$$

The non-linear element, the switch, may be treated using the describing function technique.[3] The gain-phase plot of these two functions $G(s)$ and $\frac{-1}{N(s)}$ are shown in Figure IV-20. The intersection of $G(s)$ and $\frac{-1}{N(s)}$ would indicate that oscillations would exist at infinite frequency of zero amplitude. This however, neglects the phase delay due to sampling. While the phase delay due to sampling may be introduced on the gain phase plot it is equally valid to introduce it on the phase plot alone. The limit cycle oscillation is constrained by the interrogator to have a period of integral multiples of the clock time, ΔT. The stored velocity, V_s, is proportional to the magnitude of the limit cycle and it is therefore, desirous to have it small. The phase delay due to the sampler is $\frac{2\pi}{n}$ where n is the number of ΔT's per cycle in the limit cycle. The addition of the phase delay to G(s) shows intersections with $\frac{-1}{N(s)}$ and thus satisfies the conditions for $G(s) = \frac{-1}{N(s)}$. The moding or limit cycle may be described as 1:1 where there is one sampling pulse per half cycle. A n:n mode is where there are n sampling pulses per half cycle. The phase delays are shown as lines of phase shift at frequency $\omega = \frac{\pi}{n\Delta T}$. The illustrated graph shows as possible limit cycles either the 1:1 or 2:2 mode, and it is impossible to have a 3:3 or higher mode limit cycle operation.

It is possible here to decrease the moding by decreasing the ratio of J/C. For a physical instrument the value of J is fairly firmly established and not much alteration is possible. However, a fairly wide viscosity range of damping fluid is possible. This would seem to indicate that increasing the damping would reduce the limit cycle to its lowest mode. Such is usually the case; however, one must now consider the signal-to-noise ratio of the instrument. As the damping increases the float motion decreases. It becomes then a question of the smallest detectable float angle. That is to say what is the minimum angle from null at which you can positively identify the float angle as positive or negative.

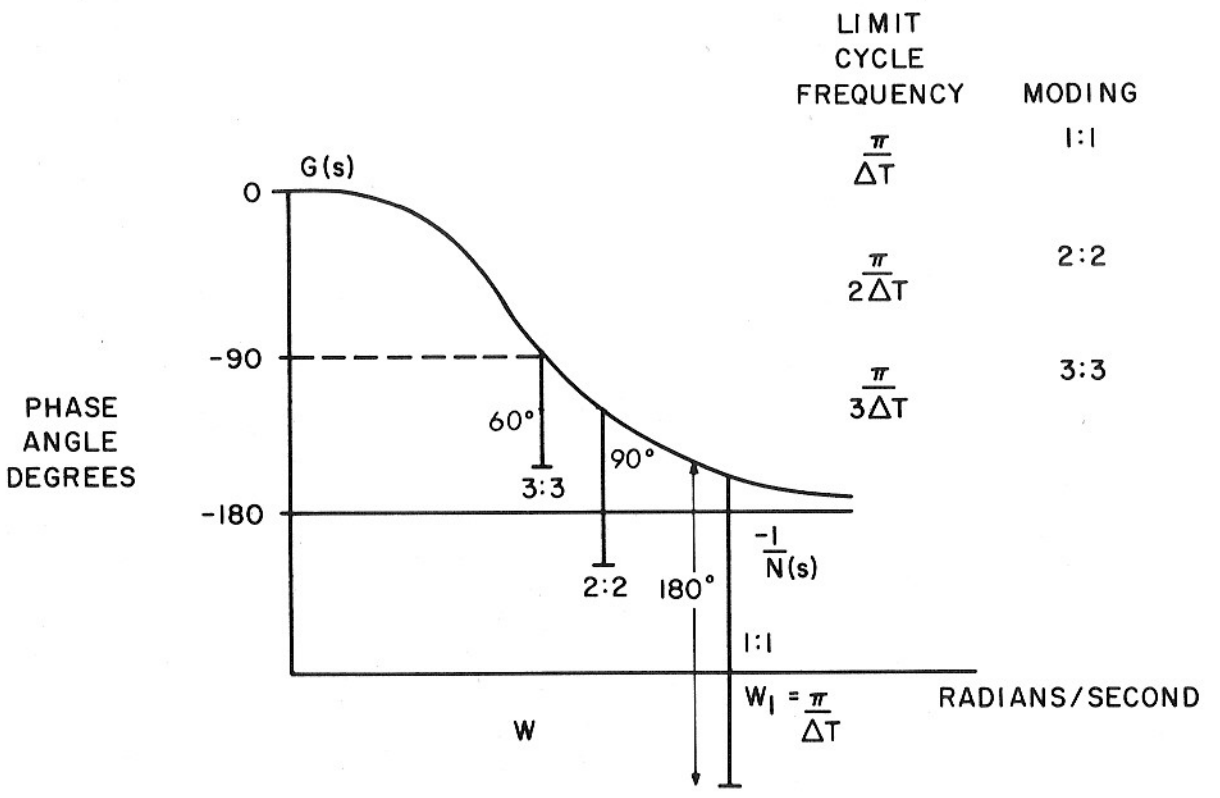

SAMPLER PLACE DELAY = $\frac{2\pi}{n}$

n = NUMBER OF CLOCK INTERVALS (ΔT) PER CYCLE OF OSCILLATION

Fig. IV-20 PIPA Limit Cycle

Fig. IV-21 16 Pulsed Integrating Pendulum, Mod D

From previously, $V_s = J A_{c-f} + C A_{c-f}$ + Initial Conditions. Assuming initial conditions are zero and near null the minimum angle of detection is $A_{c-f} = A_m$. At this point the damping torque is much greater than the inertia reaction torque therefore.

$$\dot{A}_{c-f} = \frac{M_{tg}}{C} \qquad \text{(IV-6)}$$

$$V_s = \frac{J}{C} M_{tg} + C A_m \qquad \text{(IV-7)}$$

The damping for minimum stored velocity is

$$C = \sqrt{\frac{J M_{tg}}{A_m}} \qquad \text{(IV-8)}$$

This relationship is heuristically correct in that a smaller detectable angle (higher signal-to-noise ratio) will permit increased damping. While decreasing J will reduce the float time constant. Increasing torque, M_{tg}, will in the same time interval increase float angle equivalent to reducing A_m.

PIP - The physical inertial component, the pendulum (PIP), is a single-degree-of-freedom pendulum. The pendulum is floated both to reduce friction uncertainty and to provide damping about all three axes. The output axis damping is to provide good dynamic behavior while the damping about the other axes are to provide geometrical stabilization of the float with respect to the case. This is necessary to assure stability of performance. There is an electromagnetic suspension system called ducosyn to provide both axial and radial centering forces to additionally stabilize the float with respect to the case. The float is a hollow cylindrical beryllium piece with ferrite rotors cemented on each end. There is a pivot shaft used for axial and radial stops of the suspension system. The pendulosity, 1/4 gm cm, is adjusted by a pin and screw which also serve as the output axis stop limiting rotation of A_{c-f} to less than $\pm 1^{o}$. On a diameter perpendicular to the pendulous axis are two screws used to achieve flotation. Surrounding the float is the damping block. The damping fluid and the clearances between the float and the case set the damping to about 120,000 dyne cm/radian/second. Located in the damping block are four bellows for volume compensation. On each end is the end housing which has the electromagnetic suspension system on the inner rotor and the signal generator or torque generator on the outer rotor. The rotor itself is a one piece device. The torque generator is an eight pole device with windings on the even poles for negative torque and on the odd poles for positive torque. The torque is proportional by the sensitivity of the torque generator, S_{tg}, and to the square of the current. The damping fluid is the only mechanical connection between the float and the case. This has made a pendulum with a friction uncertainty level of less then 0.02 dyne centimeters when only the suspensions and signal

generator are excited. The float inertia about the pivot as output axis is approximately 14 gm/cm^2. The float time constant, J/C, is about 100 microseconds. The pendulum time constant for the float with the input reference axis and output axis perpendicular to gravity is eight minutes.

The signal generator is an eight pole device with limitations identical to those of the torque generator. It uses a primary excitation and a differential center tapped secondary. The signal generator is resistive and capacitive tuned for a second order system damping ratio of nearly unity and natural frequency slightly greater than the carrier frequency. This prevents excessive phase delays of the signal generator from affecting the moding and yet reduces high frequency noise generated and picked up in the signal generator.

The effects of an elastic restraint, K, may be seen by considering the basic equation:

$$J \ddot{A}_{I-f} + C \dot{A}_{c-f} + K A_{c-f} = M_{tg} + ml\, a_{IA} \qquad \text{(IV-9)}$$

K = elastic restraint coefficient

for the average values of the angle $\bar{A}_{c-f}$. This eliminates the limit cycle when considering small inputs.

$$J \dddot{\bar{A}}_{c-f} + C \ddot{\bar{A}}_{c-f} + K \dot{\bar{A}}_{c-f} = ml\, a_{IA} \qquad \text{(IV-10)}$$

Considering the inertia reaction torque small with respect to the damping torque and elastic restraint torque

$$C \ddot{\bar{A}}_{c-f} + K \dot{\bar{A}}_{c-f} = ml\, a_{IA}$$

$$\bar{A}_{c-f} = \frac{ml\, a_{IA}}{K} \left[1 - e^{-\frac{Kt}{C}}\right] \qquad \text{(IV-11)}$$

This is to say a finite positive K reduces the average angle through which the float will rotate. Any elastic restraint will alter the time at which an output, ΔV, will be indicated. A positive K will increase the apparent integration time and a negative K will decrease the apparent integration time. The limiting positive K case shows an interesting concept. Consider that there corresponding to a ΔV an equivalent average float angle ΔA.

$$\Delta \dot{A} = A\, \Delta T = \frac{M_{tg}}{C} \Delta t \qquad \text{(IV-12)}$$

For a steady state case as $t \longrightarrow \infty$

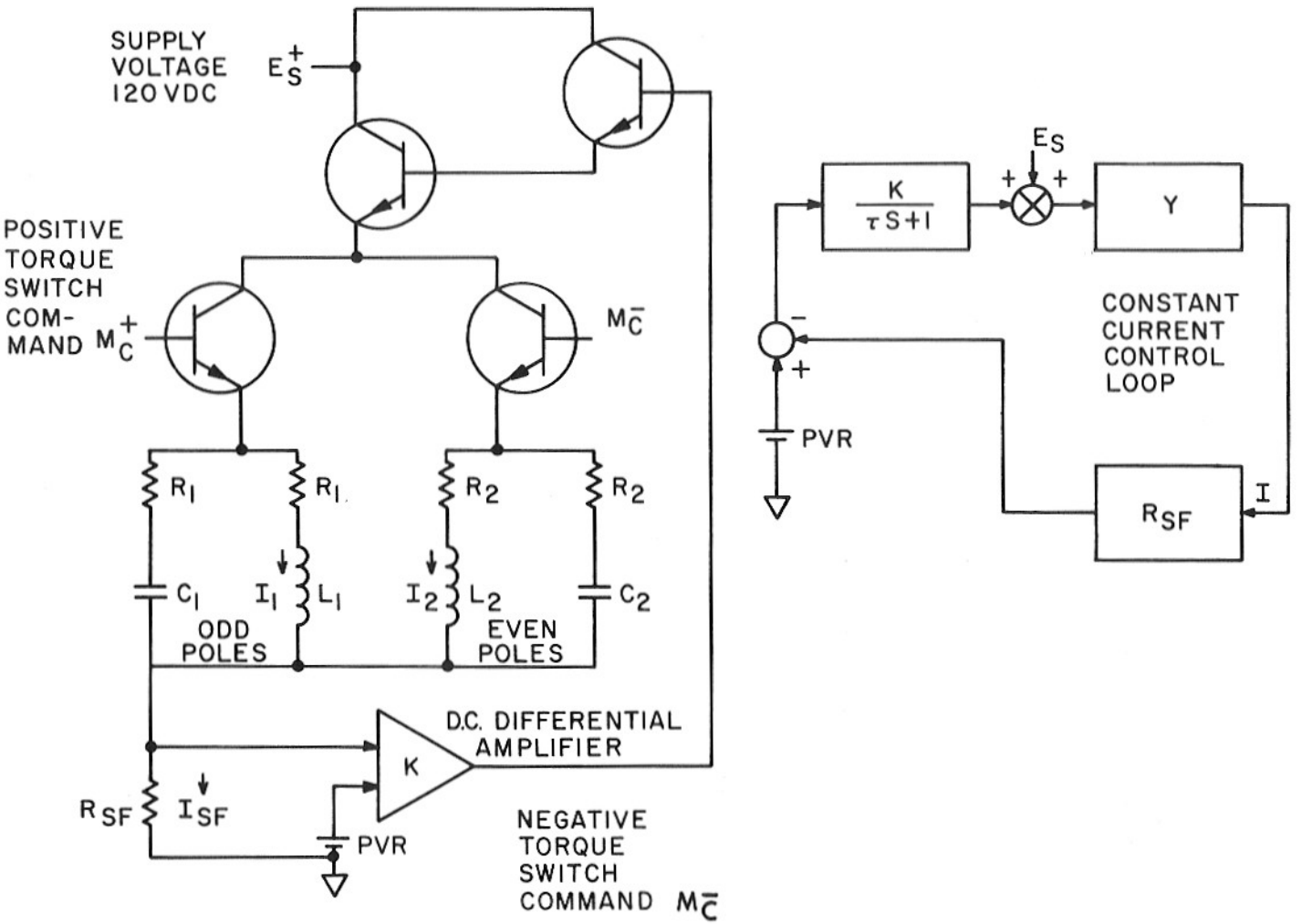

Fig. IV-22 Current Control and Current Switch

A_{c-f} = ΔA as a necessary condition for integrating an input acceleration

$$\frac{ml\ a_{IA}}{K} = \frac{M_{tg}}{C}\ \Delta T$$

or

$$K = \frac{ml\ a_{IA}}{M\ \Delta T} \quad C = \frac{C\ a_{IA}}{\Delta V} \tag{IV-13}$$

This shows the minimum detectable input acceleration under conditions of a finite elastic restraint. Furthermore, this shows that increasing C reduces the effect of elastic restraint. We again return to the criteria of the minimum detectable angle A_m. For the optimum damping

$$K \leqq \frac{a_{IA}\ ml}{\Delta T} \sqrt{\frac{J}{A_m\ M_{tg}}} = \frac{a_{IA}}{\Delta V} \sqrt{\frac{J\ M_{tg}}{A_m}} \tag{IV-14}$$

Refer to Fig. IV-22. The torque generator flats to create a pseudo-salient pole are not just a single planar surface. There a multiple planar surfaces near the cylindrical rotor portion designed to reduce the elastic restraint to a negligibly small value. The accelerometer itself is the best means of measuring the elastic restraint coefficient. The minimum detectable acceleration is below 0.05 cm/sec^2

Scale Factor and Bias - The constant current loop with the reference and switching is shown in Fig. IV-23. A d.c. differential amplifier compares the voltage drop across a scale factor resistor with that of a precision voltage reference. The torque generator of the PIP is a V connected microsyn torque generator. Torque is developed proportional to the difference of the squares of the current in odd poles and even poles. Switching of current is controlled by appropriate drive voltages to the basis of the switch transistors for M_c^+ or M_c^-. The network of resistances and capacitance associated with each torque are chosen to make the impedance of the switched network resistance. That is to say $\frac{L_1}{R_1} = R_1 C_1$. This for the amplifier has the output impedance always resistive. As will be shown later it is desirable to have the voltage across the compensated windings as high as possible to reduce the current rise time. However, the upper limit is controlled by the breakdown voltage of transistors used in this switching application. The amplifier gain is chosen to reduce the effects of supply voltage disturbances to acceptable limits. The dynamic response of the amplifier is chosen to reduce the current squared effects due to supply voltage changes to an acceptable vaue.

$$\frac{I}{E} = \frac{\frac{Y}{Y\ R_{SF}\ K}}{\tau\ s + 1} + 1$$

For a change of E_s of 10% or 12 volts the gain, K = 200,000, is determined such that the current changes are less than 10 ppm*. Dynamic response of the control loop, principally controlled by the amplifier, is set to minimize current transients. Loop compensation is required for stability and also to control current transients due to switching. The current rise time for the current in the torque generator (I_1, I_2) is desired to be a small as possible. The amplifier, drive impedance is tuned to be resistive to minimize current transients. Thus the torque generator impedance is tuned to be resistive with the addition of a resistor and capacitor. The current rise time, L_1/R_1 is then controlled by R_1 since L_1 is controlled by the torque generator. The current requirement, I_{SF}, is determined from the scale factor requirement and the torque generator sensitivity. This leaves only the supply voltage, E_S, as the variable for R_1 determination. The desire to increase R_1 is then determined as a compromise between the desire to increase R_1 and the limitation of E_S for voltage breakdown reasons, V_{CE}, of the current control transistors. Based upon the current state of the art for reliable producible transistors 120 volts was chosen as a suitable compromise. In the steady state case this leaves about 80 volts across C_1 or C_2.

The stability of the current loop is determined by two other important items, the scale factor resistor and the voltage reference, call Precision Voltage Reference, PVR. Precision resistors with low temperature coefficients are commerically available. The method used for setting the desired conductance is to normalize all PVR's to a particular value, 6,000 volts and then adjust two fixed values R_L and R_{SF} with the ratio $\frac{R_L}{R_{SF}}$ between 100 and 1300:

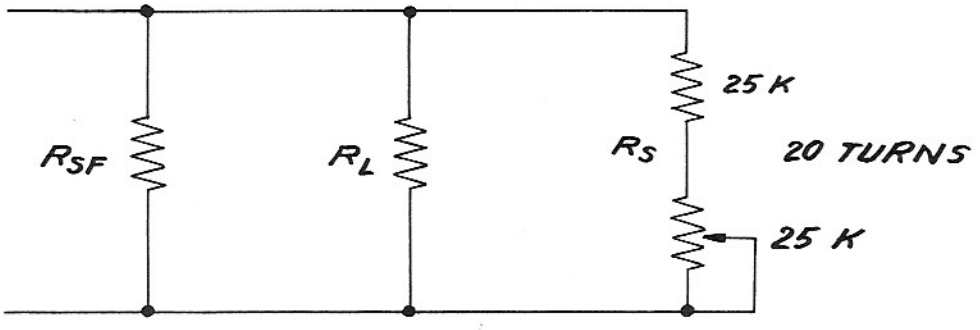

With this method precision adjustment is possible by the use of the potentiometer. Resistance stability is generally better than 3 ppm/year with temperature coefficients of less than 3 ppm/C^o deviation. The Precision Voltage Reference

* This work done by James L. Sitomer, Instrumentation Laboratory.

is a cascaded zener diode voltage source.

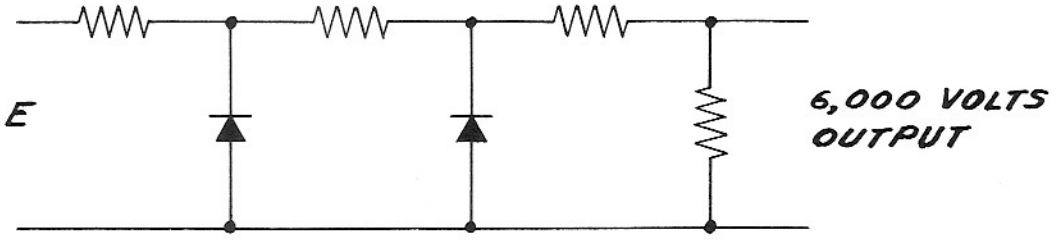

The second stage is chosen for a voltage where the temperature coefficient of the diode is nearly zero. This is slightly greater than 6 volts which is the point at which the temperature coefficient changes sign. The resistor divider network on the output is the normalization of the PVR to 6,000 volts. Voltage deviations of the PVR are less than 10 ppm/year with changes due to temperature less than 3 ppm/C^{o}. This then forms the major portion of the constant current loop.

As in any accelerometer the stability of parameters in one of the most important considerations. From previously

$$SF = \frac{S_{tg}\, i^2\, \Delta T}{ml}$$

$$dSF = \frac{\partial SF}{\partial S_{tg}}\, dS_{tg} + \frac{\partial SF}{\partial i}\, di + \frac{\partial SF}{\partial\, \Delta T} + \frac{\partial SF\ d\,ml}{\partial\ ml} \qquad \text{(IV-16)}$$

$$\frac{dSF}{SF} = \frac{dS_{tg}}{S_{tg}} + \frac{2\, di}{i} + \frac{d\Delta T}{\Delta T} - \frac{d\,ml}{ml}$$

This is the fundamental relation describing stability of the scale factor. Mechanization is required to minimize these changes. The pendulosity is very stable. The current control has been previously described to minimize $\frac{di}{i}$. A single computer pulse train is used for switching the torque. As a precaution against any modulation of the switching pulse amplitude and the resulting timing changes a second pulse train, interrogration pulse, which precedes by a short time the switching pulse is used to set the state of the gates to allow switching with the switch pulse. This eliminates any apparent elastic restraint effects which might result from summing the float angle information with the switching pulse.

The primary scale factor stability parameter is the torque generator sensitivity.

The torque generator sensitivity is proportional to the permeability and inversely proportional to the gap. The gap is controlled by the magnetic suspension

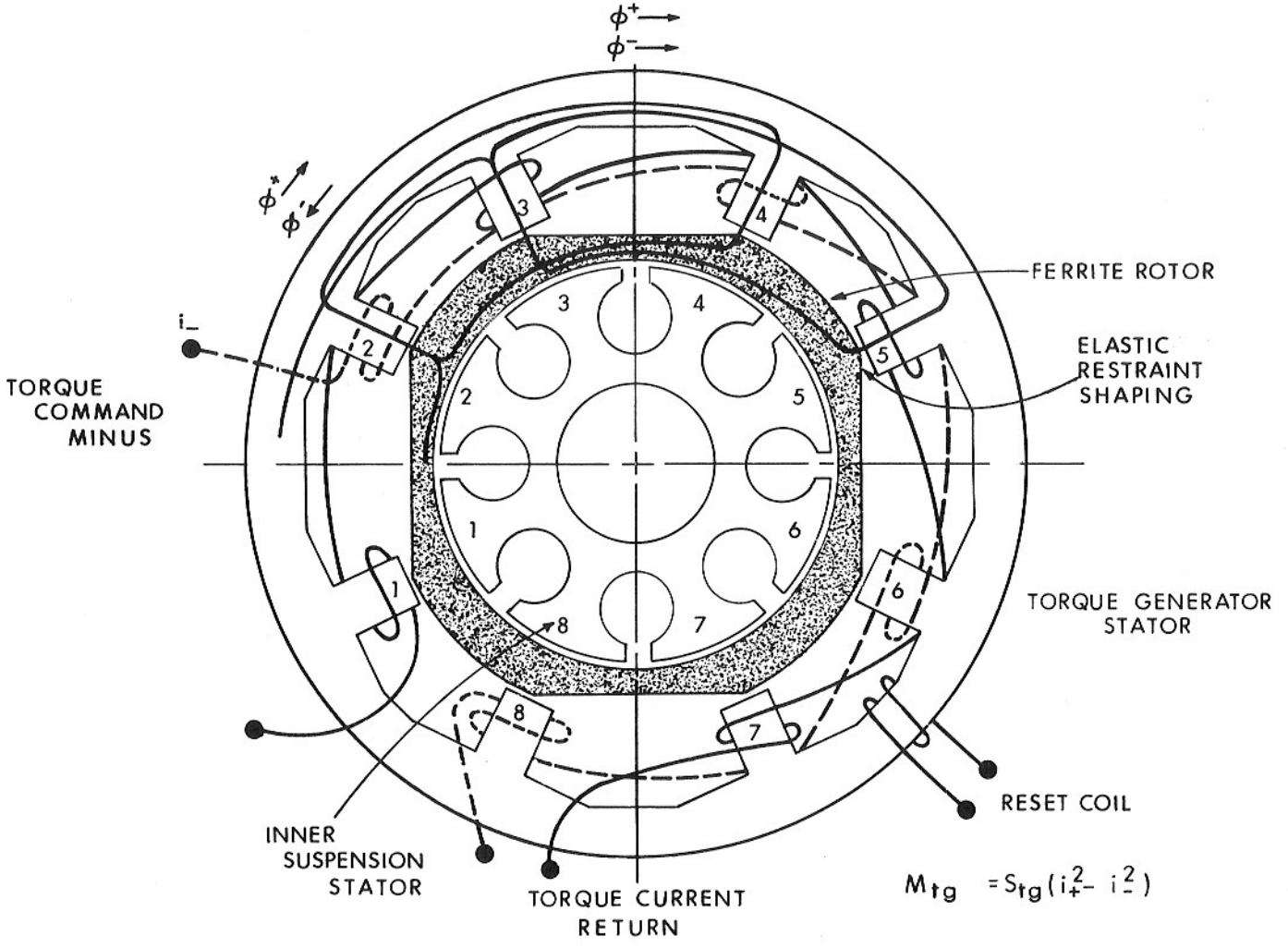

Fig. IV-23 Apollo 16 PIP Mod D Torque Generator Schematic Diagram

system with radial force restraints of 3 grams force/10^{-4} inches and about 1/20 this stiffness for the axial restraint.

The stabilization of the permeability requires a number of things. First a review of the torque generator will show that at the stator locations between poles there are alternate locations of d.c. and a.c. flux. These d.c. flux regions are locations where memory can be maintained. This memory may be erased by the reset coil which has an a.c. flux in the back iron of the stator. The rotor memory is erased by the suspension system through the one piece rotor.

The quality of any accelerometer is determined by its performance stability. The bias, a_b, of the accelerometer (output with no input) and its stability has another relationship. The torque generator is compensated to the resistive. Upon switching,the current in one winding decays exponentially, while it rises exponentially in the other winding. The torque is proportional to the difference of the square of the current.

$$M_{tg} = S_{tg} \ (i_1^2 - i_2^2 \ )$$

If M_{tg} is integrated over one limit cycle period and averaged the bias due to the torque generator is obtained.

$$M_{avg} = \frac{1}{2n \ \Delta T} \int_o^{2n \ \Delta T} S_{tg} \ (i_1^2 - i_2^2 \ ) \ dt = ml \ a_b$$

Thus bias acceleration, a_b, is proportional to difference to the current rise time.

$$a_b = \frac{\Delta V}{\Delta T} \ \frac{\tau_2 - \tau_1}{2n \ \Delta T} \qquad \text{(IV-17)}$$

It is important to have these two times identical or the bias would be a function of the period 2n ΔT. The accelerometer itself is the best instrument to use to adjust these two rise times to be identical. By introducing a phase delay (decreasing the damping for example) the moding may be altered. Then the change in bias is proportional to the current time constant differences.

The other parameter of primary significance in an accelerometer is the alignment and stability of the input axis. The mounting flange can be seen on the view of the pendulum. On that flange is a slot. The surface of the flange and the slot then form the reference alignment directions. The stable member contains the mounting surface and pin with the proper tolerances. The input axis is aligned about the output axis by rotating the PIP with respect to the slot. The mounting flange contains two rings which have mating spherical surfaces. Alignment of the input axis about the pendulous reference axis is obtained by sliding between these surfaces. The two rotations are uncoupled for small rotations. The pendulum is thus prealigned prior to

its assembly into the IMU. Like the gyro it also contains a module of the necessary suspension capacitors and other normalizing components. For alignment reasons this module fastens into the stable member and not the pendulum.

CHAPTER IV-3

THE COUPLING DATA UNIT (CDU)

The Coupling Data Unit, provides the central angle junction box between the IMU, Optics, Computer and the certain portions of the spacecraft analog electrical interfaces. There are three basic portions of the CDU. They are angle read system or analog to digital conversion process, the digital to analog conversion process, and a portion of the moding controls for the guidance system. The analog to digital system will be covered in some detail and other portions only mentioned.

Analog to Digital Conversion - Angle information is stored in a two speed resolver system of a control member, for example a gimbal axis or an optical axis (see Figure IV-24.) The output of the resolver is proportional to $\sin\theta$, $\cos\theta$, $\sin n\theta$, $\cos n\theta$, where n is a binary number. It is a common technique to have both the single speed and multiple speed resolver use the same iron and utilize a single excitation winding. The second excitation winding space phased 90^{o} with respect to the primary excitation is used for electrical zero adjustment. The elements of the angle read system are an analog multiplication of the resolver output, an analog summation, a sampler and quantizer, a storage counter to control the analog multiplication, and a.c. switches controlled by the counter to gate inputs to the analog multiplies.

The equation mechanized is:

$$\sin\theta\ \cos\psi\ -\cos\theta\ \sin\psi\ =\ \sin\ (\theta-\psi) \qquad \text{(IV-18)}$$

$$\cos\theta\ \cos\psi\ +\sin\theta\ \sin\psi\ =\ \cos\ (\theta-\psi) \qquad \text{(IV-19)}$$

Where ψ is a quantized angle is increments of 22 1/2 electrical degrees, and

θ is the angle of the control member

As shown in Figure IV-25 this output is summed with a quantized linear interpolation of difference between $\sin(\theta-\psi)$ and θ. The selection of the quantized angle ψ and the quantized linear interpolation angle ϕ, is based upon the contents of an angle counter register. The angle counter inputs are gated by the phase the summed voltages. Thus when the contents of the counter are equal to the control member angle:

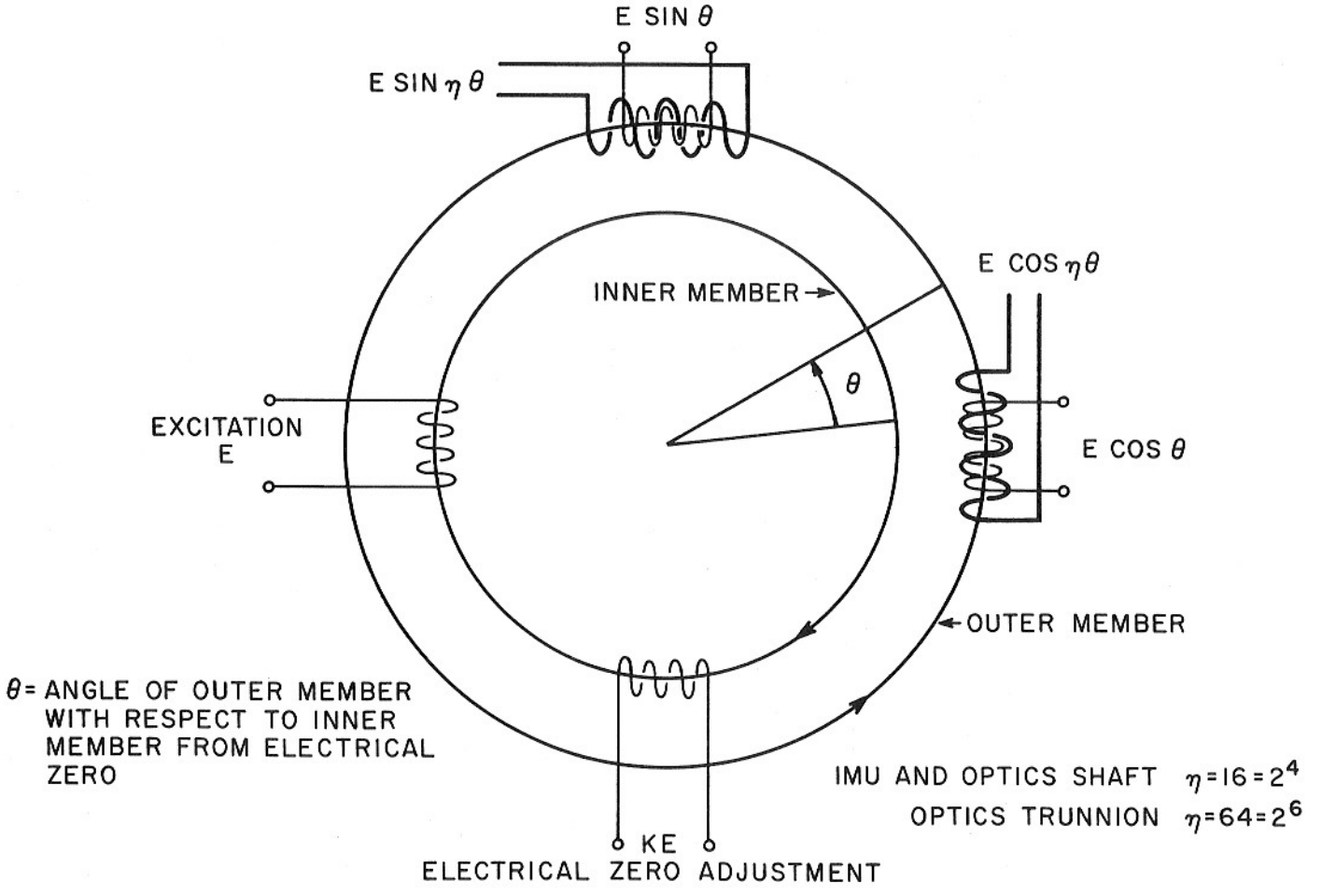

Fig. IV-24 Resolver Schematic

$$\sin(\theta - \psi) + K \cos(\theta - \psi) = 0 \qquad \text{(IV-20)}$$

The inputs to the counter are angle increments of the control member and these are parallel fed to the computer where the same control member angle information is stored.

Analog multiplication of the resolver sin θ and cos θ voltage is

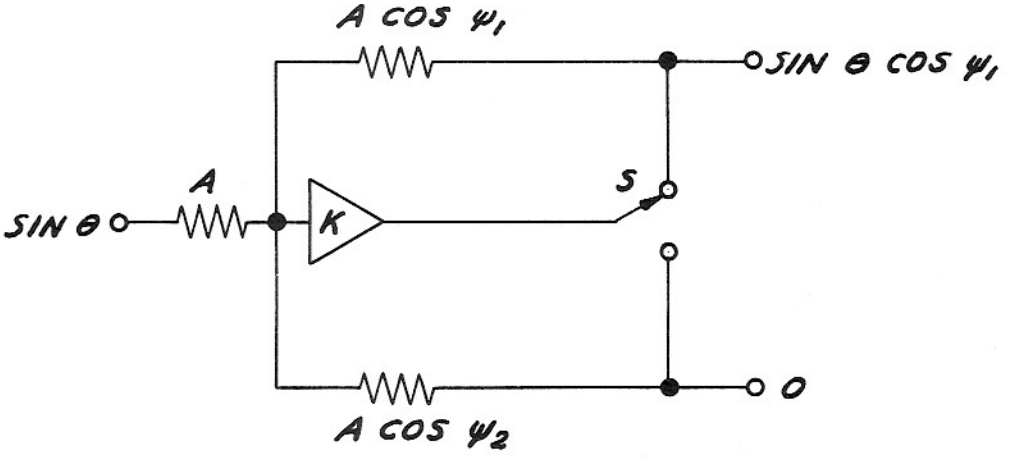

accomplished by the use of an ac operational amplifier with the ratio of the feedback resistor to the input resistor equal to the cosine of the angle ψ_1. S is an ac transistorized switch gated closed or open by contents of the angle counter resistor The switch is in series with the feedback resistor to take advantage of the high impedance open condition and low impedance closed condition which makes the impedance equivalent to a portion of the amplifier gain, K. Since the switch is effectively a single pole double throw switch the output of the open side differs from zero only by the input signal divided by the amplifier gain. Using the technique of transistorized ac switches and operational amplifiers the read system is mechanized. The read counter contains 16 bits. The lowest order bit is used to eliminate transmitting any limit cycle operation to the computer and thus creating unnecessary activity. The four highest order bits are used for quadrant selection and multiplication of the single speed resolver (ψ_1). In addition, the bits 2^9 - 2'' are used as an approximate linear interpolation of the single speed resolver to within 2.81° of the actual angle. The multiple speed resolver (sixteen speed) is the precision angle transmitting device. The zero-to-peak errors of this resolver are less than 20 seconds of arc. There is crossover between the sixteen speed and the single speed resolvers to assure synchronization of the reading of sixteen speed resolver within the proper cycle. The lowest order bits are a linear interpolation of error using the voltage of the cos $(\theta - \psi)$ as a source. This voltage has the same phase relation as the sin $(\theta - \psi)$ of the sixteen speed resolver and is

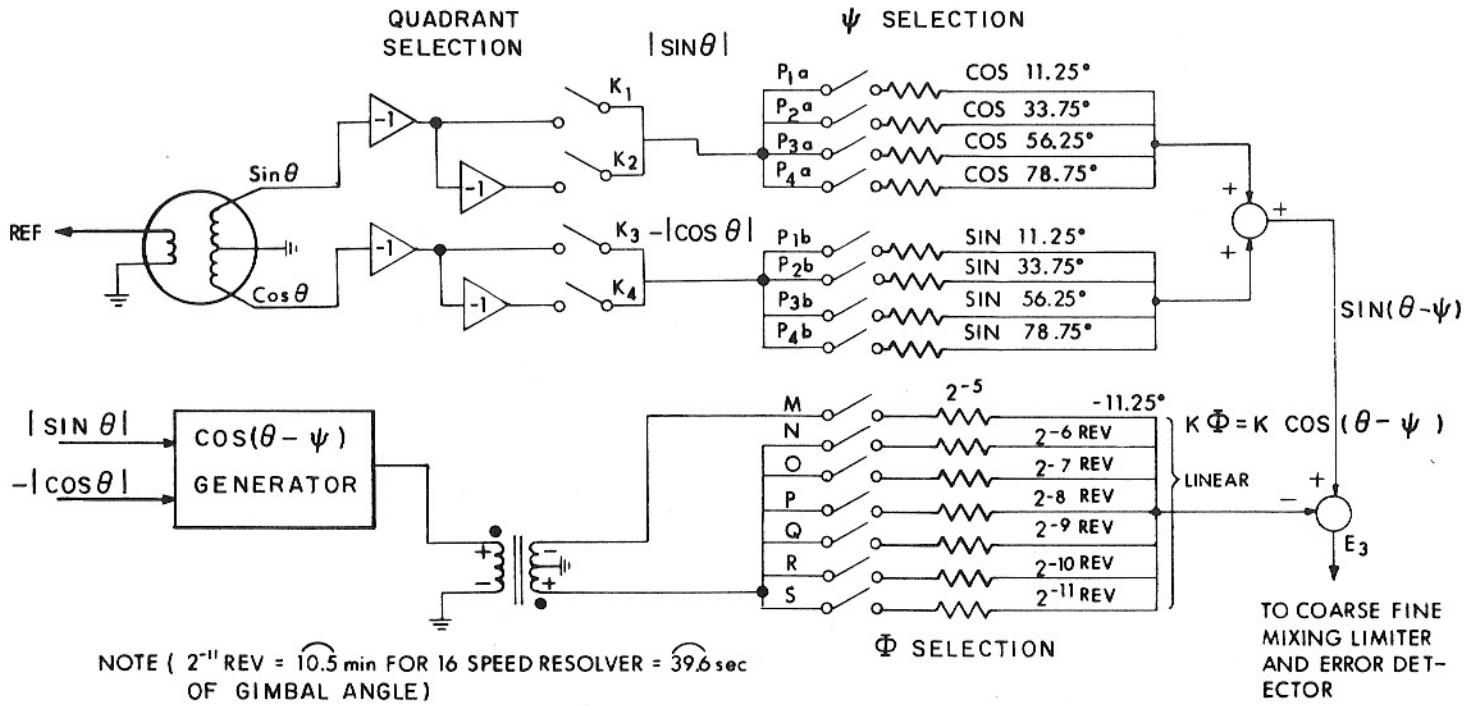

Fig. IV-25 Selection Logic - 16 Speed Resolver Digitizing Loop

scaled correctly by the resolver attenuation.

Referring to Fig. IV-26 the input to the error detector is the sum of the single speed multiplication, the sixteen speed multiplication and the linear interpolation. There is a coarse-fine mixing network to assure synchronization and angle measurement using the precision resolver. The error detector contains an active feedback quadrature rejector network which for large error signals will not introduce dynamic errors for reading the angle, but for small errors will yield the proper precision. The output of the error detector is fed to both the rate selection logic and up-down counter logic. The contents of the counter are used to control the a. c. switches for the multiplication of the resolver voltages and the linear interpolator.

The error detector has three-state or ternary logic. The lowest order pulse rate command to the counter is 800 pulses per second. Using this as the lowest order assures switching of equal multiples of the resolver carrier frequency, 800 cps. This prevents rectification of the switched signal and altering of the dynamic operation of the read system.

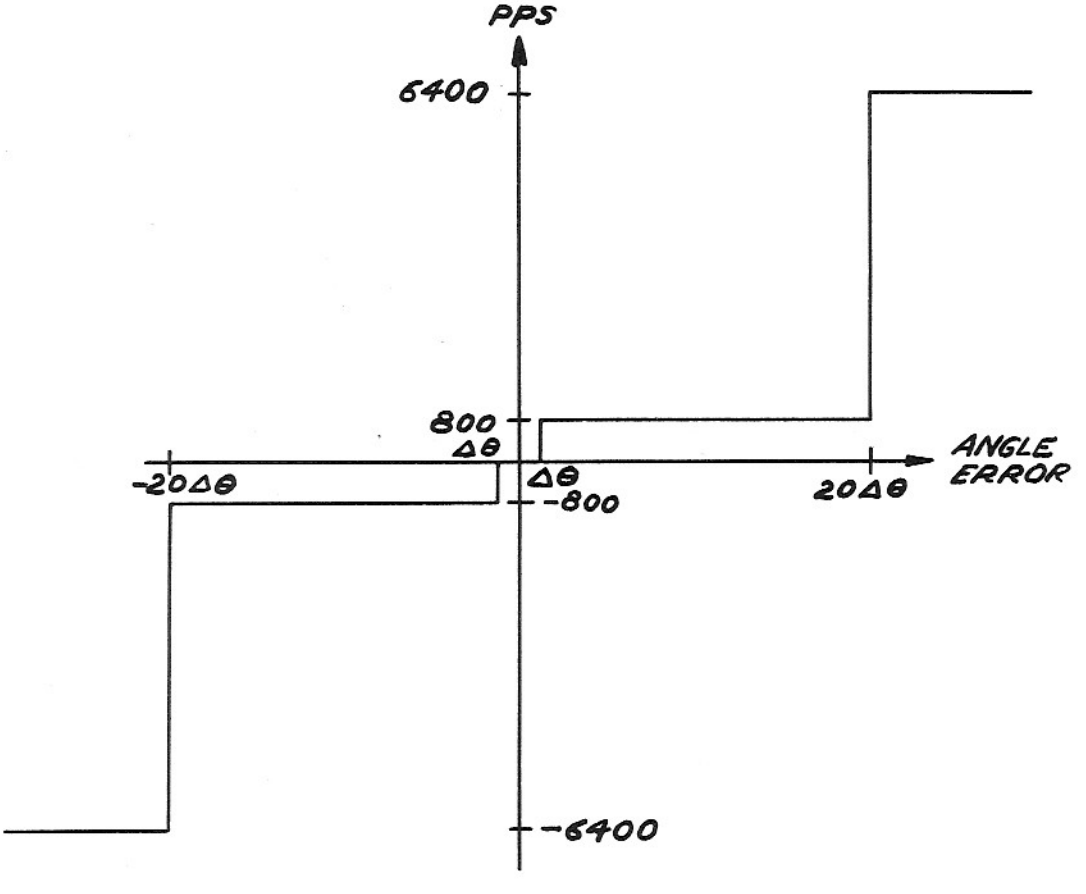

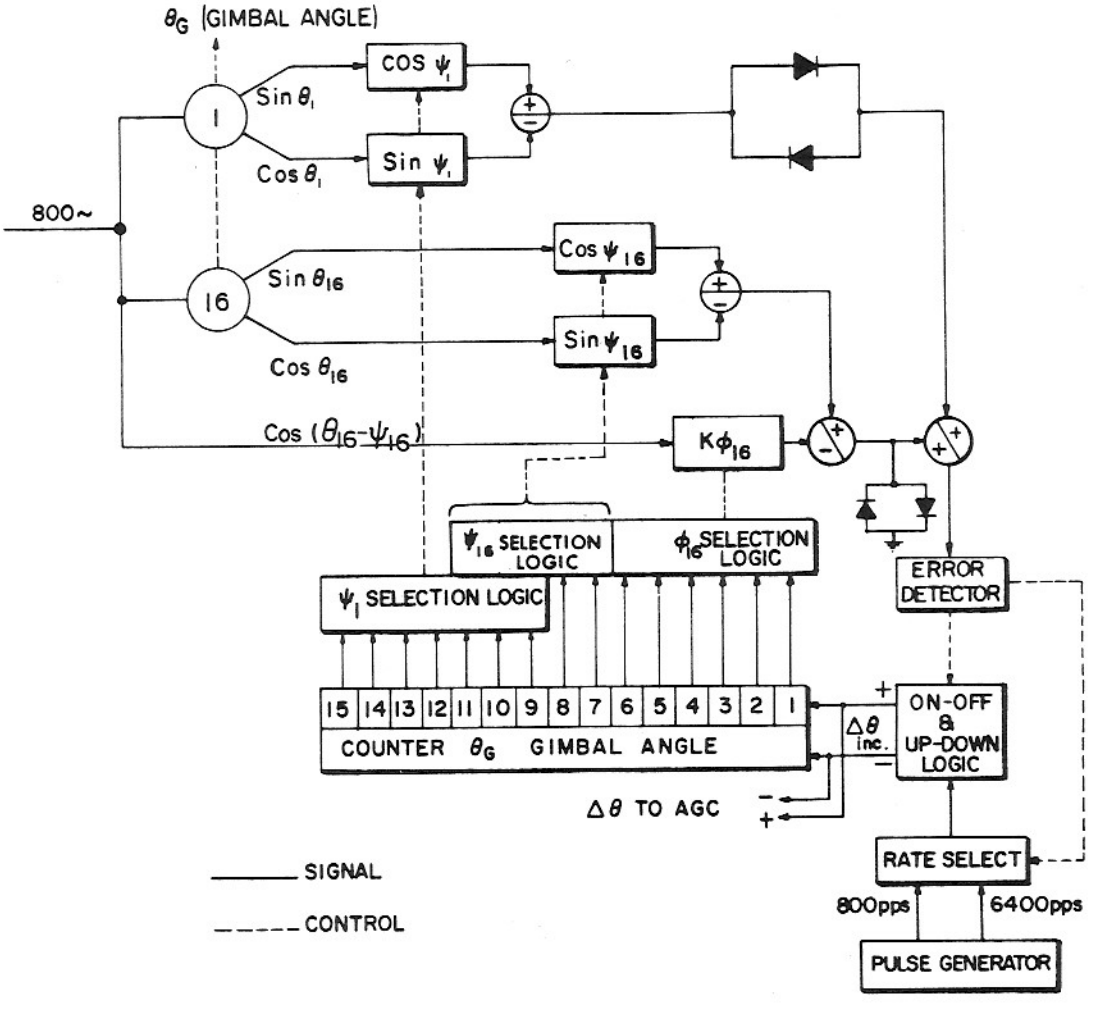

Fig. IV-26 Coarse-Fine Mixing (1 and 16 Speed Resolver

The high speed rate following command reduces dynamic error for high angular velocity inputs and the low speed command rate reduces the limit cycle error.

The linear interpolation constant K is adjusted to minimize the peak error

$$E = \sin(\theta - \psi) - K \cos(\theta - \psi) \qquad \text{(IV-21)}$$

By suitably choosing K the error for the speed resolver system can be reduced to less than 10 sec arc. For a 64 speed system as used on the optics trunnion this error is reduced to less than 3 sec arc.

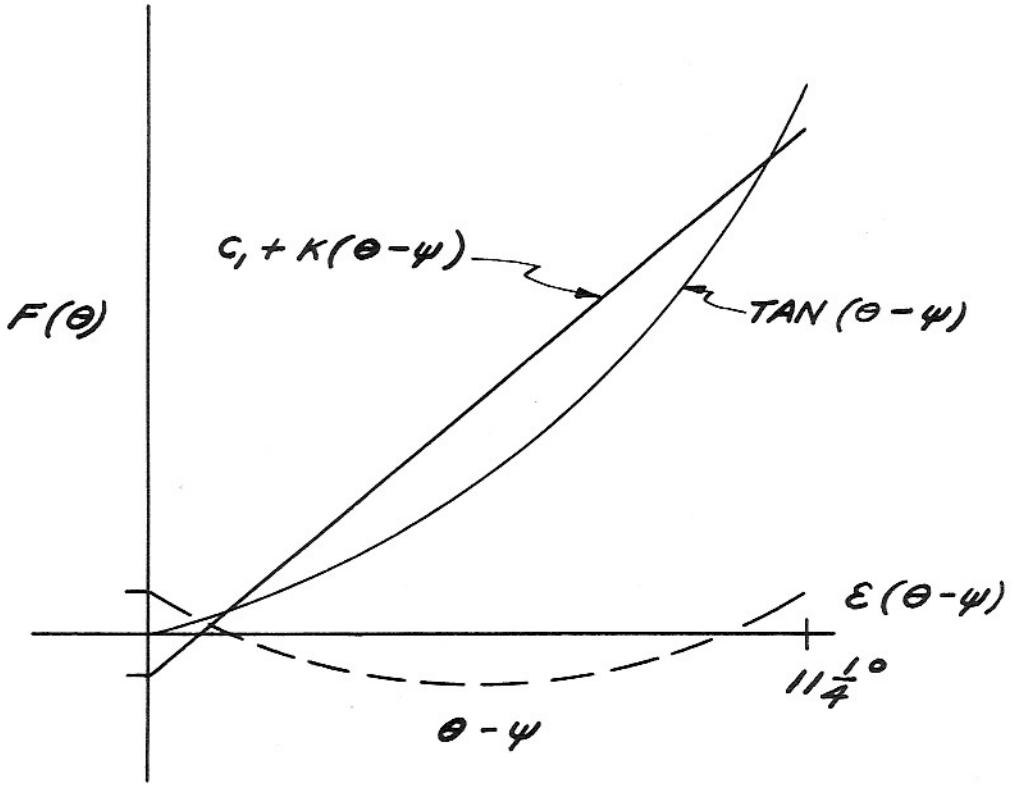

In addition, a bias is added to further reduce the errors over the entire range of linear interpolation. This results in a system whose errors are within the predicted errors.

All digital functions including the memory are mechanized with the three input NOR gate, a silicon semiconductor micro-integrated circuit. This is the same element used in the computer. Direct coupled transistorized logic is used throughout. A multiple phase clock system, generated within the CDU and synchronized

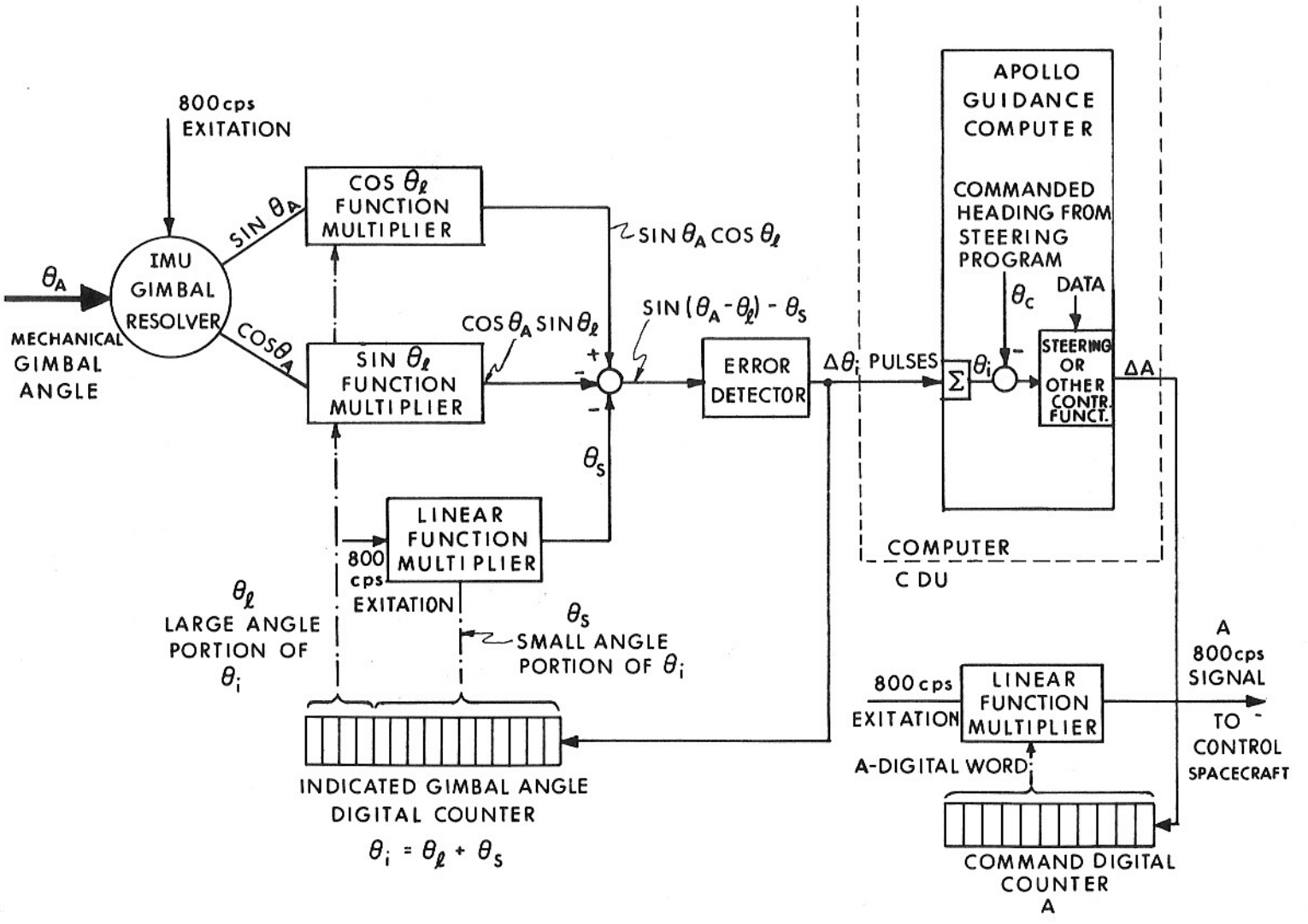

Fig. IV-27 Electronic Coupling Data Unit Schematic

to the guidance computer, is used to control all functions.*

Moding and Digital to Analog Conversion - The guidance computer serves as the important link between the spacecraft and the sensing device. All angle transformations are made by the guidance computer based upon IMU gimbal angles or optics angles. For any steering function utilizing the IMU, the computer through the use of knowledge of the gimbal angles provides steering and attitude commands to the spacecraft via the digital to analog converter. The angle information is always stored in the resolvers and no mechanical rezeroing of the IMU is necessary to establish within the counter the IMU gimbal angle within the uncertainty of the resolver, the error of the read system and the bit size of the analog to digital converter.

The digital to analog converter system is required to accept digital commands from the guidance computer and generate analog voltages (a. c. and d. c.) proportional to these commands. The error angle counter is an eight bit up-down counter. Computer commands are stored in this counter. The counter is logically controlled to prevent it from being reset to zero in the event it is commanded to more than 2^8 increments. The analog error signals are developed by an 800 cps source gated by the counter contents through a resistance ladder to the input of an operational amplifier. For polarity reversal by switching is used to command the 0 phase or π phase 800 cps input to the ladder. All analog voltages used as steering commands to the LEM, Spacecraft or other portions of the Apollo launch vehicle are d. c. isolated from the guidance system either by transformers or an isolated demodulator.

The moding of the system is almost entirely controlled by the computer. Provision is made for two modes to be controlled by the astronaut. One mode is the cage function. In the event of a spacecraft tumble and loss of attitude, provision is made for the astronaut to cage the IMU gimbals with respect to the spacecraft after he has first stabilized the craft. This then gives him a means of obtaining a new reference in a very short time. The other manual mode is similar in that with the computer not operating he can use the same switch to cage the IMU with respect to the spacecraft, release it, and again use the IMU as an attitude reference.

All other moding is controlled by the computer as can be seen from Fig. IV-28 for the IMU. Optics moding has more manual control and is shown in Fig. IV-29. This moding will be described elsewhere. There are a number of interesting modes possible because of the flexibility of the CDU. The Coarse Align Mode, that of commanding the IMU gimbal angles by the resolvers, is rate controlled to limit angular velocity input to the gyroscopes. The input to the error detector is sum-

*This work is by Robert Crisp and Glenn Cushman, MIT Instrumentation Laboratory

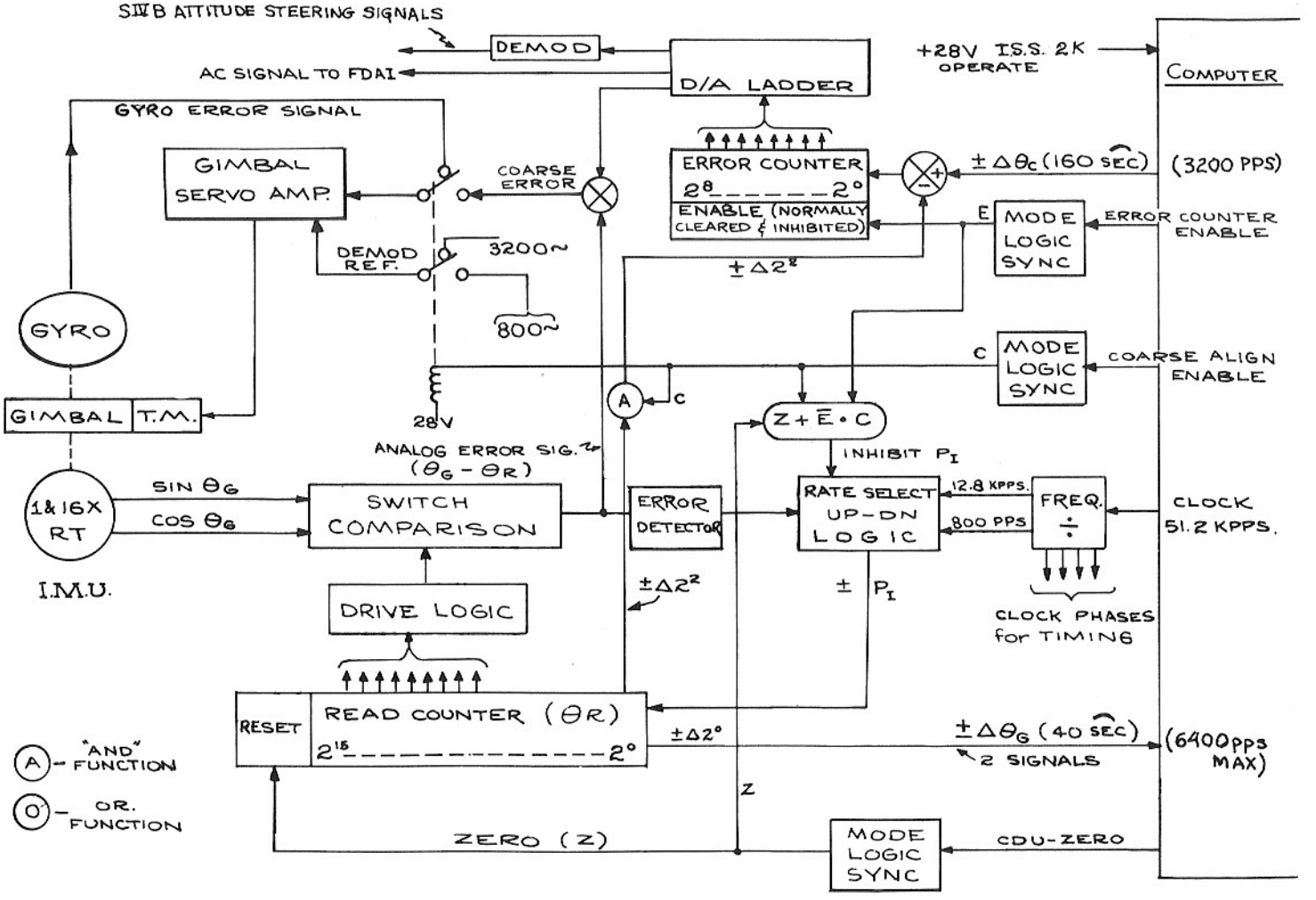

Fig IV-28 IMU-CDU Moding

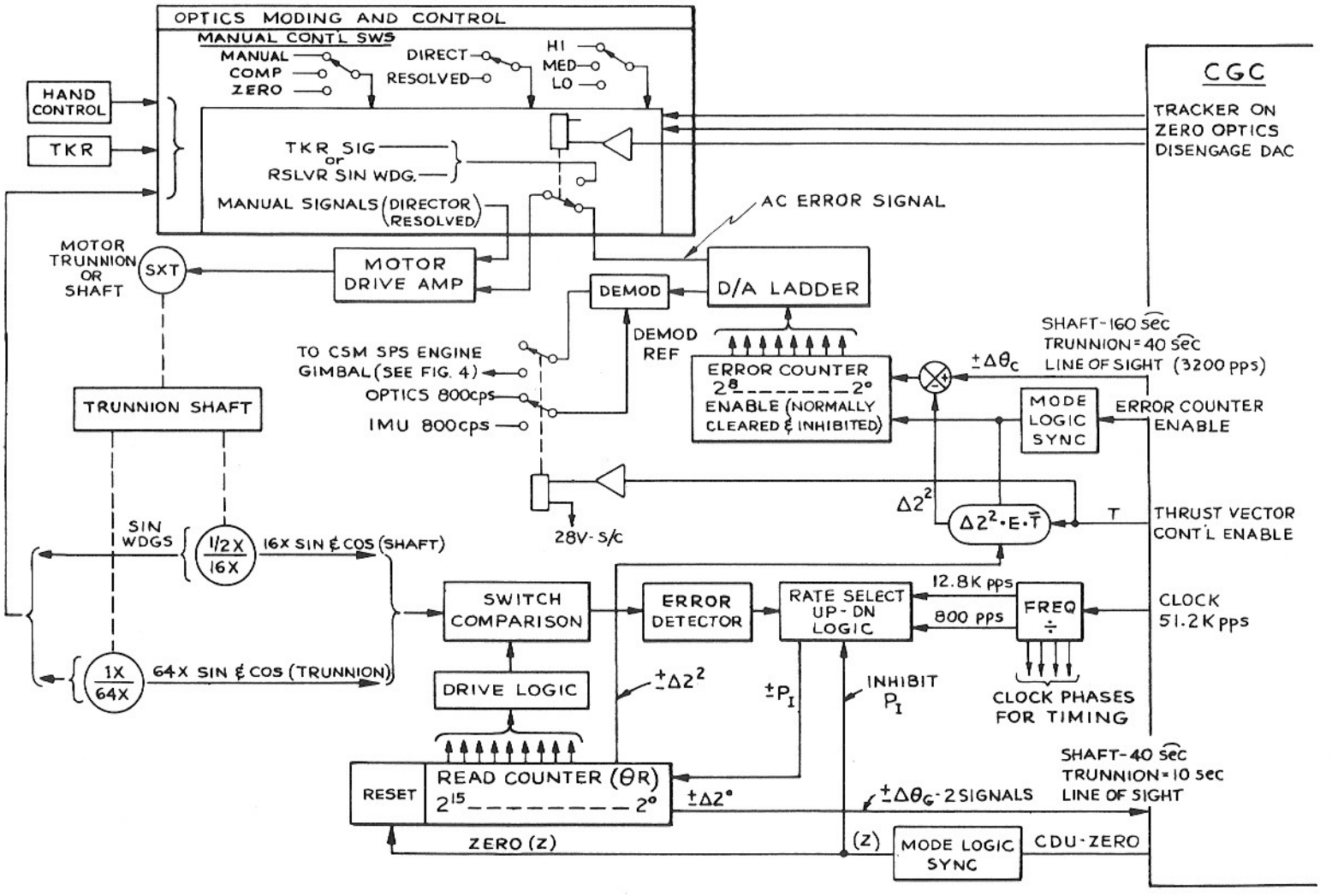

Fig. IV-29 Optics-CDU Moding (CSM only)

med with the analog command from the computer to provide stable operation. The gimbal angle pulse increments from the read system are used as feedback pulse to the error angle counter.

BIBLIOGRAPHY

1. C. S. Draper, W. Wrigley, and L. R. Grohe, "The Floating Integrating Gyro and Its Application to Geometrical Stabilization Problems on Moving Bases," Institute of the Aeronautical Sciences Preprint 503, presented January 25, 1955.

2. P. J. Gilinson Jr., W. G. Denhard, and R. H. Frasier, "A Magnetic Support for Floated Inertial Instruments." Report No. R-277 Instrumentation Laboratory, MIT, Cambridge, Massachusetts, April 1960.

3. Thomas Freud Wiener, "Theoretical Analysis of Gimballess Inertial Reference Equipment Using Delta-Modulated Instruments, MIT, Cambridge, Massachusetts, Sc D Thesis.